Cell Reports

Article

The subunits of IL-12, originating from two distinct cells, can functionally synergize to protect against pathogen dissemination *in vivo*

Graphical abstract

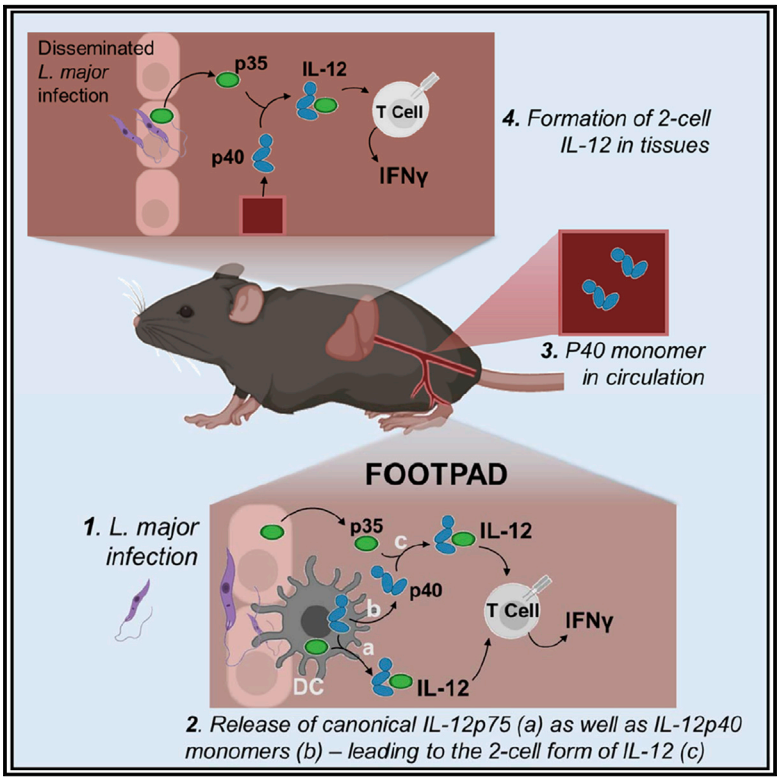

Highlights

- Both p35 and p40 subunits of IL-12 are required to differentiate IFNγ-producing T cells
- p35 and p40 produced by two different cells can collaborate to drive T cell responses
- The two-cell IL-12 activity requires hematopoietic p40 but can use stromal p35
- Two-cell IL-12 activity is useful for controlling pathogen dissemination *in vivo*

Authors

Allison N. Gerber, Kaveh Abdi, Nevil J. Singh

Correspondence

Allison.Gerber@som.umaryland.edu (A.N.G.), kabdi@niaid.nih.gov (K.A.), nsingh@som.umaryland.edu (N.J.S.)

In brief

The innate cytokine IL-12 is a critical enhancer of IFNγ production. Gerber et al. show that IL-12 activity can result from two distinct cells contributing different subunits of IL-12 independently, *in vivo*. This collaborative, two-cell version of IL-12 could limit pathogen dissemination to tissues distant from the primary infection site.

Gerber et al., 2021, Cell Reports *37*, 109816
October 12, 2021
https://doi.org/10.1016/j.celrep.2021.109816

CellPress

Cell Reports

CellPress
OPEN ACCESS

Article

The subunits of IL-12, originating from two distinct cells, can functionally synergize to protect against pathogen dissemination *in vivo*

Allison N. Gerber,[1,*] Kaveh Abdi,[2,*] and Nevil J. Singh[1,3,*]

[1]Department of Microbiology & Immunology, University of Maryland School of Medicine, 685 West Baltimore Street, HSF1, Room 380, Baltimore, MD 21201, USA

[2]Laboratory of Immunogenetics, National Institute of Allergy and Infectious Diseases, NIH, Rockville, MD 20850, USA

[3]Lead contact

*Correspondence: Allison.Gerber@som.umaryland.edu (A.N.G.), kabdi@niaid.nih.gov (K.A.), nsingh@som.umaryland.edu (N.J.S.)

https://doi.org/10.1016/j.celrep.2021.109816

SUMMARY

Cytokines are typically single gene products, except for the heterodimeric interleukin (IL)-12 family. The two subunits (IL-12p40 and IL-12p35) of the prototype IL-12 are known to be simultaneously co-expressed in activated myeloid cells, which secrete the fully active heterodimer to promote interferon (IFN)γ production in innate and adaptive cells. We find that chimeric mice containing mixtures of cells that can only express either IL-12p40 or IL-12p35, but not both together, generate functional IL-12. This alternate two-cell pathway requires IL-12p40 from hematopoietic cells to extracellularly associate with IL-12p35 from radiation-resistant cells. The two-cell mechanism is sufficient to propel local T cell differentiation in sites distal to the initial infection and helps control systemic dissemination of a pathogen, although not parasite burden, at the site of infection. Broadly, this suggests that early secretion of IL-12p40 monomers by sentinel cells at the infection site may help prepare distal host tissues for potential pathogen arrival.

INTRODUCTION

Interleukin (IL)-12 and IL-23 are members of a family of heterodimeric cytokines that play critical roles in regulating the differentiation of the immune response toward distinct effector pathways. IL-12 promotes interferon (IFN)γ secretion by natural killer (NK) cells and T cells, while IL-23 enhances IL-17 production (Tait Wojno et al., 2019). They are also unique among cytokines, as each of these is a heterodimer assembled from proteins encoded by two distinct genetic loci (Gubler et al., 1991; Sieburth et al., 1992). The formation of functional IL-12 or IL-23 requires a common IL-12p40 (p40) subunit that covalently associates with either the IL-13p35 (p35) or IL-23p19 (p19) subunit, respectively (D'Andrea et al., 1992; Oppmann et al., 2000). However, the secretion of IL-12 is canonically thought to rely on p40 and p35 being expressed and assembled within a single myeloid cell (typically dendritic cells [DCs] or macrophages). For instance, innate activation of DCs by pathogen-associated molecular patterns (PAMPs) or damage-associated molecular patterns (DAMPs) leads to the upregulation of transcripts for both subunits (Hayes et al., 1995). The subsequent assembly and secretion of the heterodimers are controlled by post-translational checkpoints (Carra et al., 2000; Jalah et al., 2013; Reitberger et al., 2017; Yoon et al., 2000). Importantly, p35 is not secreted alone and requires binding to p40 for correct folding and secretion (Reitberger et al., 2017). The teleological significance of two distinct genetic loci contributing to a tightly regulated single-cell product is not clear.

Importantly, despite this co-dependence on p40 for functional cytokine generation, p35 is widely expressed, while p40 expression is typically limited to DCs and macrophages (Carra et al., 2000; D'Andrea et al., 1992). p40 can also be released from these hematopoietic cells as a monomer and is routinely found in great excess over IL-12 in serum and culture supernatants (Abdi et al., 2006, 2014; Trinchieri, 2003). The precise biological significance of secreted p40 monomer is not yet clear, although recent studies indicate immunomodulatory properties. The p40-p40 homodimer can inhibit the IFNγ-promoting activity of IL-12 (Cooper and Khader, 2007), but the amounts of p40 monomer far exceeds this form, too. Intriguingly, at least *in vitro*, we previously reported that p40 and p35 can assemble to form functionally active IL-12 (Abdi et al., 2014). If this mechanism operates *in vivo*, it will add a layer to current models for bridging the innate and adaptive systems. Significantly, this model would suggest that two cells, one hematopoietic (expressing p40) and the other potentially non-hematopoietic (expressing p35), functionally cooperate to determine the trajectory of T cell differentiation in contrast to the single-cell dictation currently predicted by the intracellular assembly model.

To evaluate the different mechanisms by which IL-12 can be generated physiologically, we used a mixed bone marrow chimera strategy where the production of p40 or p35 is separated to different cellular compartments. In this model, cells in

the chimeras contain IL-12p40$^{-/-}$ (p40$^{-/-}$) or IL-12p35$^{-/-}$ (p35$^{-/-}$) cells such that any cell can either make p40 or p35, but not both. Despite this separation, we found that active IL-12 is available for T cell differentiation, validating this method for IL-12 formation *in vivo*. We also found that hematopoietic cells are the necessary source of p40 secretion to synergize with p35, expressed by radiation-resistant cells from the non-hematopoietic compartment, for the formation of two-cell IL-12. This two-cell method of IL-12 formation amplified effector IFNγ responses in antigen-specific T cells during immunization and in response to a *Leishmania major* infection in a polyclonal T cell population. Furthermore, we showed that the two-cell IL-12 was physiologically distinct from the canonical form and plays a major role in controlling parasite dissemination to distal sites but not the primary infection site. Taken together, these data highlight an alternate mechanism by which DCs and stromal cells collaboratively drive T cell differentiation and effector function.

RESULTS

T cell differentiation to IFNγ production is disrupted in p40$^{-/-}$ and p35$^{-/-}$ mice

The biological function of IL-12 *in vivo* is in promoting the differentiation of IFNγ-producing innate and adaptive cells. While there is considerable literature showing how cytokines such as IL-18 and IL-15 as well as T cell receptor (TCR) signaling pathways themselves influence the initial differentiation of IFNγ-producing cells (Denton et al., 2007; Matson and Singh, 2020; Müller et al., 2001; Tubo and Jenkins, 2014), the role of IL-12 in setting up a feedback loop amplifying this effector mechanism is critical in many responses (Trinchieri, 2003). Immune responses to parasites such as *Leishmania* are particularly relevant (Park et al., 2000). The differentiation of T cells during *Leishmania* infection of mice was historically used to outline the original Th1/Th2 paradigm (Heinzel et al., 1989; Scott et al., 1988). In a C57BL/6 (B6) background, the strong differentiation of T cells to an IFNγ-secretion phenotype is associated with better clearance of the subcutaneous infection by *L. major* while BALB/c animals make an IL-4-dominant, non-resolving response (Fowell and Locksley, 1999). The production of IFNγ by T, NK, or NKT cells in this context was largely dependent on IL-12 from innate sources (Afonso et al., 1994; Sypek et al., 1993). Thus, subcutaneous *L. major* infections are not cleared in IL-12p40 knockout (KO) (B6.129S1-*Il12b*^{tm1Jm}/J, referred to as p40$^{-/-}$) animals, where, even in a B6 background, the response to *Leishmania* proceeds similarly to that in the BALB/c mice (Park et al., 2000). Therefore, we first validated requirements for p40 and p35 in clearing dsRed *L. major* infections using respective knockout mice on a B6 background (Figure 1). Wild-type B6 (WT) mice began to clear lesions (marked by reduced swelling of the footpads) by 25 days, while both p40$^{-/-}$ and p35$^{-/-}$ (the IL-12p35$^{-/-}$ strain [B6.129S1-*Il12a*^{tm1Jm}/J], referred to as p35$^{-/-}$ here) animals continued to swell (Figures 1A and 1B). *L. major* infection of both WT and p35$^{-/-}$ mice resulted in systemic p40 release (Figure 1C), and similar to our previous studies with lipopolysaccharide (LPS) challenge (Abdi et al., 2006), only a fraction of this amount was part of the heterodimeric IL-12 cytokine (Figure 1D). The spleen and draining popliteal lymph node (dLN) of p35$^{-/-}$ and WT animals also secreted p40 in *ex vivo* cultures, without additional pattern-recognition receptor (PRR) stimulation (Figures S1D and S1E). Taken together, these data indicate that, as we previously reported with endotoxin challenge (Abdi et al., 2006), a footpad infection with *Leishmania* also results in the systemic release of p40.

In this model, IL-12 is typically required for the induction of IFNγ from NK, NKT, and T cells. Accordingly, about 5.2% (±0.76%) of the previously activated (marked by high levels of CD44) CD4 T cells and 13% (±2.1%) of the CD44^{hi} CD8 T cells from WT animals produced IFNγ while those were reduced to 0.37% (±0.06%) CD4 and 0.23% (±0.03%) CD8 in p40$^{-/-}$ animals and 0.8% (±0.02%) CD4 and 1.06% (±0.05%) CD8 in p35$^{-/-}$ mice (Figures 1E, 1H, S1B, and S1C). This also represented an antigen-specific deficit since lymphocytes from various tissues restimulated with soluble *Leishmania* antigen (SLA) *in vitro* for 48 h also showed lower IFNγ secretion in p40$^{-/-}$ or p35$^{-/-}$ animals (Figure 1I). Notably, the loss of p40 or p35 does not completely abrogate all of the IFNγ production by T cells. Yet, this is to be expected, as the initial upregulation of IFNγ can be stimulated by other cytokines as well, mainly IL-18 (Koutoulaki et al., 2010). However, IL-12 is more important for the amplification of the IFNγ response, as IFNγ has a positive feedback loop on the expression of both p40 and p35 (Abdi et al., 2006; Liu et al., 2003).

Finally, we validated that the role of p40 and p35 in the generation of an IFNγ response was an antigen-specific phenomenon, rather than *L. major* specific. This was done using a defined antigen-specific T cell population, lymphocytic choriomeningitis virus (LCMV)-specific TCR-transgenic SMARTA CD4 T cells, transferred into either p40$^{-/-}$ or WT mice and challenged with peptide/LPS. *Ex vivo* restimulation of these T cells confirmed that IL-12 is critical for the differentiation of SMARTA T cells to produce IFNγ (Figures 1I and 1J), similar to the behavior of polyclonal T cells during *Leishmania* infection (Figures 1A–1G).

Administration of recombinant p40 allows for antigen-specific T cell differentiation

While knockout mice illustrate the need for p40 and p35 to generate biologically active IL-12-driven IFNγ production by T cells, they cannot be used to determine whether both subunits must be expressed by the same DC or macrophage (canonical IL-12) or each can come from two different cells, hereafter referred to as the "two-cell model." A prerequisite of the two-cell model is that p40 secreted by DCs should be able to interact with p35 outside the DC and combine to generate active IL-12. There is so far no *in vivo* evidence for such a functional association of these two subunits. Therefore, we evaluated this possibility using the SMARTA T cell model described above. The expectation was that the quantitative deficiency toward IFNγ production in SMARTA T cells primed in a p40$^{-/-}$ host could be complemented by the administration of exogenous recombinant p40 monomers only if the two-cell model were valid. Accordingly, we primed adoptively transferred SMARTA T cells with peptide mixed with LPS, combined with intraperitoneal (i.p.) administration of recombinant p40 (or PBS as a control) to the p40$^{-/-}$ animals (Figure 2A). The mice were treated daily for 5 days after antigen stimulation, upon which point the T cells

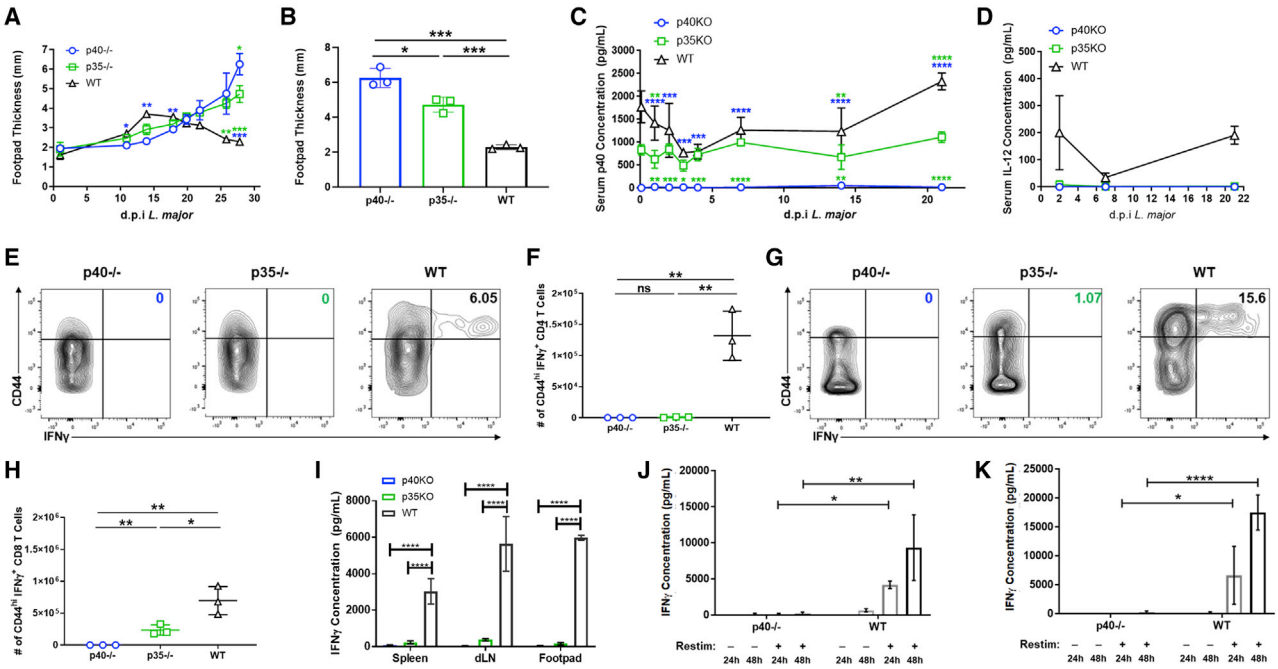

Figure 1. T cell differentiation is disrupted in p40$^{-/-}$ and p35$^{-/-}$ mice

(A–H) p40$^{-/-}$ (open circles, blue), p35$^{-/-}$ (open squares, green), and WT (open triangles, black) mice were challenged with 10^6 dsRed *L. major* parasites by intradermal injection in the footpad.

(A) Biweekly measurement of footpad thickness following appearance of lesions for p40$^{-/-}$ (open circles, blue), p35$^{-/-}$ (open squares, green), and WT (open triangles, black) through the duration of dsRed *L. major* infection (n = 3).

(B) Footpad thickness of p40$^{-/-}$ (open circles, blue), p35$^{-/-}$ (open squares, green), and WT (open triangles, black) mice 28 days after dsRed *L. major* infection (unpaired t test, n = 3).

(C and D) Infected animals were bled 4 h and at days 1, 2, 3, 4, 7, 14, and 21 after *L. major* infection. Serum (C) p40 and (D) IL-12 levels for p40$^{-/-}$ (open circles, blue), p35$^{-/-}$ (open squares, green), and WT (open triangles, black) animals were measured by ELISA (n = 3).

(E–H) Splenocytes harvested 28 days after *L. major* infection were restimulated and analyzed via flow cytometry. Gating strategy used in these panels is shown in Figure S1A.

(E) Percentage of IFNγ-producing CD4$^+$ T cells within the CD44^{hi} subset in the spleen measured 28 days after dsRed *L. major* infection (n = 3).

(F) Number of CD44^{hi}IFNγ$^+$CD4$^+$ T cells in the spleen of p40$^{-/-}$ (open circles, blue), p35$^{-/-}$ (open squares, green), and WT (open triangles, black) animals measured 28 days after dsRed *L. major* infection (unpaired t test, n = 3).

(G) Similar to (D), except CD8$^+$ T cells (n = 3).

(H) Similar to (E), except CD8$^+$ T cells (unpaired t test, n = 3).

(I) Cells from the spleen, draining popliteal lymph nodes (dLNs), and footpad were harvested 28 days after dsRed *L. major* infection and restimulated with soluble *Leishmania* antigen (SLA). Concentration of IFNγ in supernatant was measured by ELISA collected from p40$^{-/-}$ (blue), p35$^{-/-}$ (green), and WT (black, shaded) after restimulation for 48 h (unpaired t test, n = 3).

(J and K) SMARTA T cells from CD45.1$^+$ donor animals were sorted and transferred into CD45.2$^+$ p40$^{-/-}$ or CD45.1$^+$CD45.2$^+$ WT recipient animals and challenged 24 h later with $GP_{61–80}$ and LPS. 4 days after challenge, harvested cells from the spleen and LNs were restimulated with $GP_{61–80}$ *in vitro* for 24 or 48 h. Concentrations of IFNγ in the supernatant of (J) splenocyte or (K) LN SMARTA T cells transferred into p40$^{-/-}$ (open bars, blue gradient) or WT (open bars, gray gradient) animals 24 or 48 h after restimulation (n = 3) are shown.

Data in this figure are representative of two independent experiments where n refers to the number of biological replicates in each experiment. (A)–(D), (F), and (H)–(K) are displayed as mean ± SEM. *p < 0.05, **p < 0.01, ***p < 0.001, ****p < 0.0001. Colored asterisks indicate relative significance to different groups (blue is significance to p40$^{-/-}$ and green is significance to p35$^{-/-}$). Anything unmarked is considered not significant.

were harvested and restimulated *in vitro* to analyze T cell differentiation.

In response to increasing doses of $GP_{61–80}$, as seen in Figures 1J and 1K, T cells transferred into the p40$^{-/-}$ animals that received only PBS did not induce IFNγ production while the ones transferred into WT animals saw an increase of IFNγ production relative to the restimulation dose. Intriguingly, the T cells that were transferred into p40$^{-/-}$ animals that received administration of recombinant p40 saw an intermediate increase in the IFNγ production compared to the T cells in the WT animals (Figure 2B). Given previous reports about p40$^{-/-}$ animals supporting a predisposition toward a T helper (Th)2 phenotype during *Leishmania* infections, we assessed IL-4 levels in the restimulation as well. IL-4 levels were increased with a restimulation dose in the p40$^{-/-}$ animals treated with PBS but not in the WT animals, as expected. In the p40$^{-/-}$ animals that received recombinant p40, the induction of IFNγ by these T cells also resulted in a decrease in IL-4 production (Figure 2C). Levels of IL-17 were decreased in the T cells that were transferred to WT animals compared to both p40$^{-/-}$ groups (Figure 2D), and levels

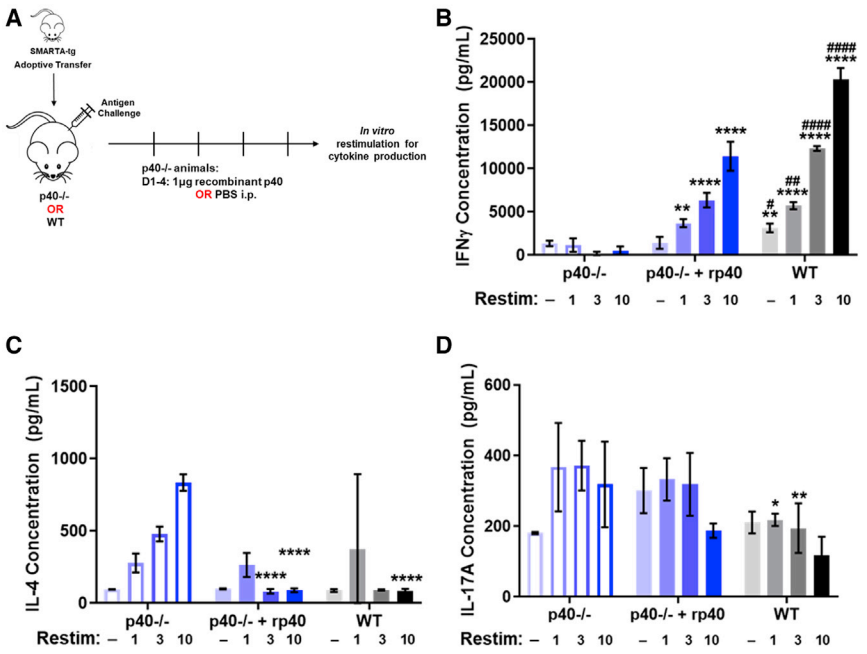

Figure 2. Administration of recombinant p40 allows for antigen-specific T cell differentiation

(A) Schematic of experimental design. SMARTA $CD4^+$ T cells from $CD45.1^+$ donors were sorted and transferred into 45.2^+ $p40^{-/-}$ animals or WT animals and challenged 24 h later with $GP_{61–80}$ and LPS. $p40^{-/-}$ recipients were divided into two groups, one that received 1 μg of recombinant p40 and the other that received sterile PBS from days 1 to 5 after transfer. SMARTA T cells were harvested from these animals at day 5 and restimulated *in vitro* to analyze for T cell differentiation by cytokine production.

(B–D) Splenocytes harvested 5 days after challenge were normalized to SMARTA T cell number and restimulated *in vitro* with $GP_{61–80}$ for 48 h. Restimulation doses are in μg. Concentration of (B) IFNγ, (C) IL-4, and (D) IL-17A in supernatant from splenocytes of SMARTA T cells transferred into $p40^{-/-}$ animals treated with PBS (left, blue open bars), $p40^{-/-}$ animals given 1 μg of recombinant p40 (middle, blue filled bars), or WT animals (right, gray filled bars) (n = 4).

Data in this figure are representative of one independent experiment where n refers to the number of biological replicates. (B)–(D) are displayed as mean ± SEM. $^{*,\#}p < 0.05$, $^{**,\#\#}p < 0.01$, $^{***,\#\#\#}p < 0.001$, $^{****,\#\#\#\#}p < 0.0001$: *significance relative to the $p40^{-/-}$ PBS-treated animals; #significance relative to the $p40^{-/-}$ animals, which received recombinant p40. Anything unmarked is considered not significant.

of IL-2 and IL-10 were unchanged between groups (Figures S2C and S2D). These data indicate that p40 and p35 do not need to be expressed in the same cell for IL-12-induced IFNγ activity to occur.

Chimeric mixing of cells singly producing either p40 or p35, but not both, allows for T cell differentiation in response to antigenic stimulation

Treatment with recombinant p40 showed that the assembly of IL-12 was not limited to a single cell in which both p40 and p35 subunits are expressed. However, this strategy did not answer whether *in vivo*, in the context of a physiological stimulation, two different cells can contribute to the subunits to make up a functional IL-12 response. To examine the potential of the two-cell model *in vivo*, we designed a chimeric strategy eliminating the ability of any given cell to make both p40 and p35 on its own (Figure 3A). In chimeric $p40^{-/-}$ animals, irradiated and reconstituted with bone marrow from $p35^{-/-}$ mice ($p35^{-/-} \rightarrow p40^{-/-}$), hematopoietic cells from the donor ($p35^{-/-}$) can make p40 but not p35. The residual host ($p40^{-/-}$) tissues, alternatively, can express p35 but not p40. This chimera would generate IL-12 only if the collaborative assembly of functional IL-12 envisioned in the two-cell model operated *in vivo*.

We first wanted to examine this using the same SMARTA T cell model. After flow cytometric analysis of chimeric mice confirming the depletion of host-derived major histocompatibility complex class II $(MHC\ class\ II)^+$ cells (Figures S3B and S3C) and subsequent reconstitution with donor cells, we used SMARTA T cells to interrogate the differentiation of naive CD4 T cells driven by IL-12 formed via two-cell assembly. SMARTA T cells were adoptively transferred to $p35^{-/-} \rightarrow p40^{-/-}$ chimeric animals and challenged with LCMV $GP_{61–80}$ peptide (with LPS adjuvant). 5 days later, splenocytes were analyzed (Figure 3). SMARTA T cells seeded and expanded to comparable levels in all chimeric hosts following antigen challenge (Figures 3B and S3F). Antigen-specific restimulation of these T cells *ex vivo* showed that WT → p40 chimeras supported strong IFNγ differentiation (Figure 3C, gray). Conversely, $p40^{-/-} \rightarrow p40^{-/-}$ chimeras were unable to promote skewing toward IFNγ production (Figure 3C, blue). Interestingly, in $p35^{-/-} \rightarrow p40^{-/-}$ chimeras, where IL-12 activity is only available through the proposed two-cell model, SMARTA cells were able to produce significant IFNγ compared to $p40^{-/-} \rightarrow p40^{-/-}$ animals (Figure 3C, green). The $p35^{-/-} \rightarrow p40^{-/-}$ chimeras also showed a higher production of IL-17A (Figure 3D, green), which can be influenced by IL-23. This suggests that in the loss of canonical IL-12 production, p40 produced by hematopoietic cells will be more available to bind p19 to form IL-23, since in this setup, both subunits can be made by the same DC. Levels of IL-4 in SMARTA T cells from WT → $p40^{-/-}$ and $p35^{-/-} \rightarrow p40^{-/-}$ chimeras were negligible, while $p40^{-/-} \rightarrow p40^{-/-}$ chimeras made significantly more (Figure 3E), confirming that IL-4 production is promoted in the absence of both canonical and two-cell IL-12 formation. These data indicate that the alternate pathway for IL-12 assembly involving two separate cells is sufficient for the differentiation of antigen-specific T cells toward IFNγ production *in vivo* after antigen-specific stimulation.

The two-cell model of IL-12 assembly allows for T cell differentiation to IFNγ during *L. major* infection

Given that the tenets of Th1/Th2 skewing and the role of IL-12 were first elucidated using *L. major* infection in mice (Afonso et al., 1994; Heinzel et al., 1989), we chose to use the same infection to evaluate the role of the two-cell model for IL-12 generation

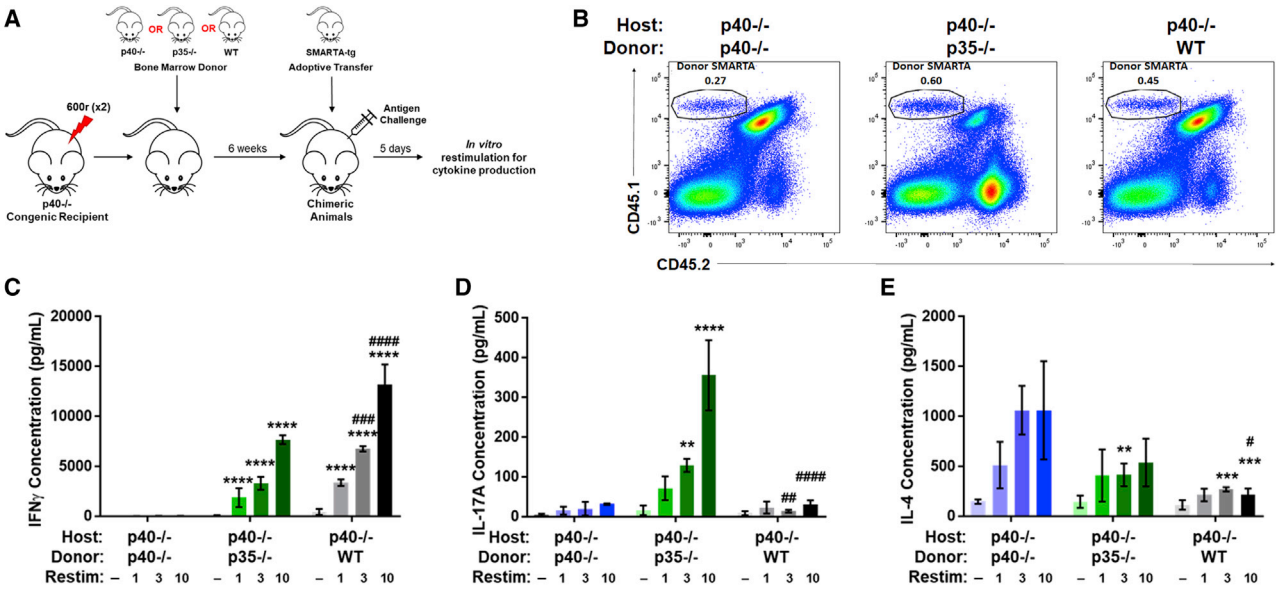

Figure 3. Chimeric mixing of cells producing either p40 or p35, but not both, still allows for T cell differentiation in response to antigenic stimulation

(A) Schematic of experimental design. Bone marrow chimeras were generated by reconstituting irradiated CD45.1$^+$CD45.2$^+$ p40$^{-/-}$ mice with bone marrow cells from CD45.2$^+$ p35$^{-/-}$ donor mice or irradiated CD45.2$^+$ p40$^{-/-}$ mice with bone marrow cells from CD45.1$^+$CD45.2$^+$ p40$^{-/-}$ or CD45.1$^+$CD45.2$^+$ WT donor mice. SMARTA CD4$^+$ T cells from CD45.1$^+$ donors were sorted and transferred into chimeric animals after reconstitution and challenged 24 h later with $GP_{61–80}$ and LPS.

(B) Identification of transferred SMARTA T cells in spleens of recipient animals 5 days after challenge (n = 3). Gating strategy for this panel is shown in Figure S2A.

(C–E) Splenocytes harvested 5 days after challenge were normalized to SMARTA T cell number and restimulated *in vitro* with $GP_{61–80}$ for 48 h. Restimulation doses are in μg. Concentrations are shown of (C) IFNγ, (D) IL-17A, and (E) IL-4 in supernatant from splenocytes of SMARTA T cells transferred into p40$^{-/-}$ host chimeras reconstituted with p40$^{-/-}$ (left, blue gradient), p35$^{-/-}$ (middle, green gradient), or WT (right, gray gradient) animals after restimulation for 48 h (n = 3). Data in this figure are representative of one independent experiments where n refers to the number of biological replicates. (C)-(E) are displayed as mean ± SEM. $^{*,\#}p < 0.05$, $^{**,\#\#}p < 0.01$, $^{***,\#\#\#}p < 0.001$, $^{****,\#\#\#\#}p < 0.0001$: *significance relative to the p40$^{-/-}$ → p40$^{-/-}$ animals; $^{\#}$relative to the p35$^{-/-}$ → p40$^{-/-}$ animals. Anything unmarked is considered not significant.

during infection response. Using the strategy outlined in the previous section, p40$^{-/-}$ chimeric mice were infected with *L. major* (Figure 4A). As expected, among T cells in *L. major*-infected WT → p40$^{-/-}$ chimeras, 9.6% (±0.93%) of the CD4 T cells produced IFNγ, which was significantly higher than that in CD4 T cells from p40$^{-/-}$ → p40$^{-/-}$ chimeras (1.6% [±0.43%]) (Figures 4B and S4B). Strikingly, in the p35$^{-/-}$ → p40$^{-/-}$ chimeras, where individual DCs cannot assemble the IL-12 heterodimer on their own, frequencies of IFNγ-producing CD4 T cells were comparable to those in WT → p40$^{-/-}$ animals, averaging 8.9% (±1.03%) (Figures 3B and S3B). The total number of IFNγ-producing CD44^{hi} CD4 T cells mirrored the pattern seen in the frequencies (Figure 4C). Similarly, for CD8s, the frequency and number of CD44^{hi} T cells producing IFNγ in WT → p40$^{-/-}$ chimeras (13.23% [±2.23%]) were higher than those in p40$^{-/-}$ → p40$^{-/-}$ (2.6% [±0.55%]) but similar to those in p35$^{-/-}$ → p40$^{-/-}$ animals (9.3% [±1.02%]) (Figures 4D, 4E, and S4C). These data suggest that two-cell formation of IL-12 is comparable to canonical IL-12 in driving differentiation of T cells toward an IFNγ response during *L. major* infection.

Similar to the data seen in the SMARTA model in Figure 3, the IL-4 responses were also affected in the chimeric mice. The p40$^{-/-}$ → p40$^{-/-}$ chimeras had increased CD4 T cell production of IL-4 while the p35$^{-/-}$ → p40$^{-/-}$ animals had similar proportions and numbers of CD44^{hi} IL-4-producing T cells to those in the WT → p40$^{-/-}$ animals (Figures S4F and S4G). Interestingly, unlike the data in the SMARTA model, the p35$^{-/-}$ → p40$^{-/-}$ animals saw no significant difference in the proportion and number of CD4 T cells producing IL-17 compared to the p40$^{-/-}$ → p40$^{-/-}$ animals (Figures S4H and S4I). This indicates that the upregulation of p19 versus p35 is context-dependent, lending further evidence for the two-cell model being a specific way for tissues to collaborate and carry out IL-12-specific activities when necessary.

In the *L. major* model, the primary site of infection is the dermis of the mouse footpad. While T cells recovered from this tissue site in p35$^{-/-}$ → p40$^{-/-}$ chimeras had increased frequencies (6.1% [±1.7%] for CD4s and 5.4% [±3.4%]) in CD8s) of IFNγ production relative to p40$^{-/-}$ → p40$^{-/-}$ chimeras (1.7% [±0.5%] for CD4s and 0.5% [±0.7%] in CD8s), they did not reach the levels seen in WT → p40$^{-/-}$ chimeras (26.2% [±7.1%] for CD4s and 13.4% [±3.1%] in CD8s) (Figures 4F, 4I, S4D, and S4E). Cells taken from various tissue sites and restimulated with SLA for 24 or 48 h confirmed the disparity in IFNγ production between p40$^{-/-}$ → p40$^{-/-}$ and WT → p40$^{-/-}$ animals in an antigen-specific manner. In the antigen-specific restimulation, the IFNγ production in p35$^{-/-}$ → p40$^{-/-}$ chimeras maintained an intermediate phenotype between p40$^{-/-}$ → p40$^{-/-}$ and WT → p40$^{-/-}$

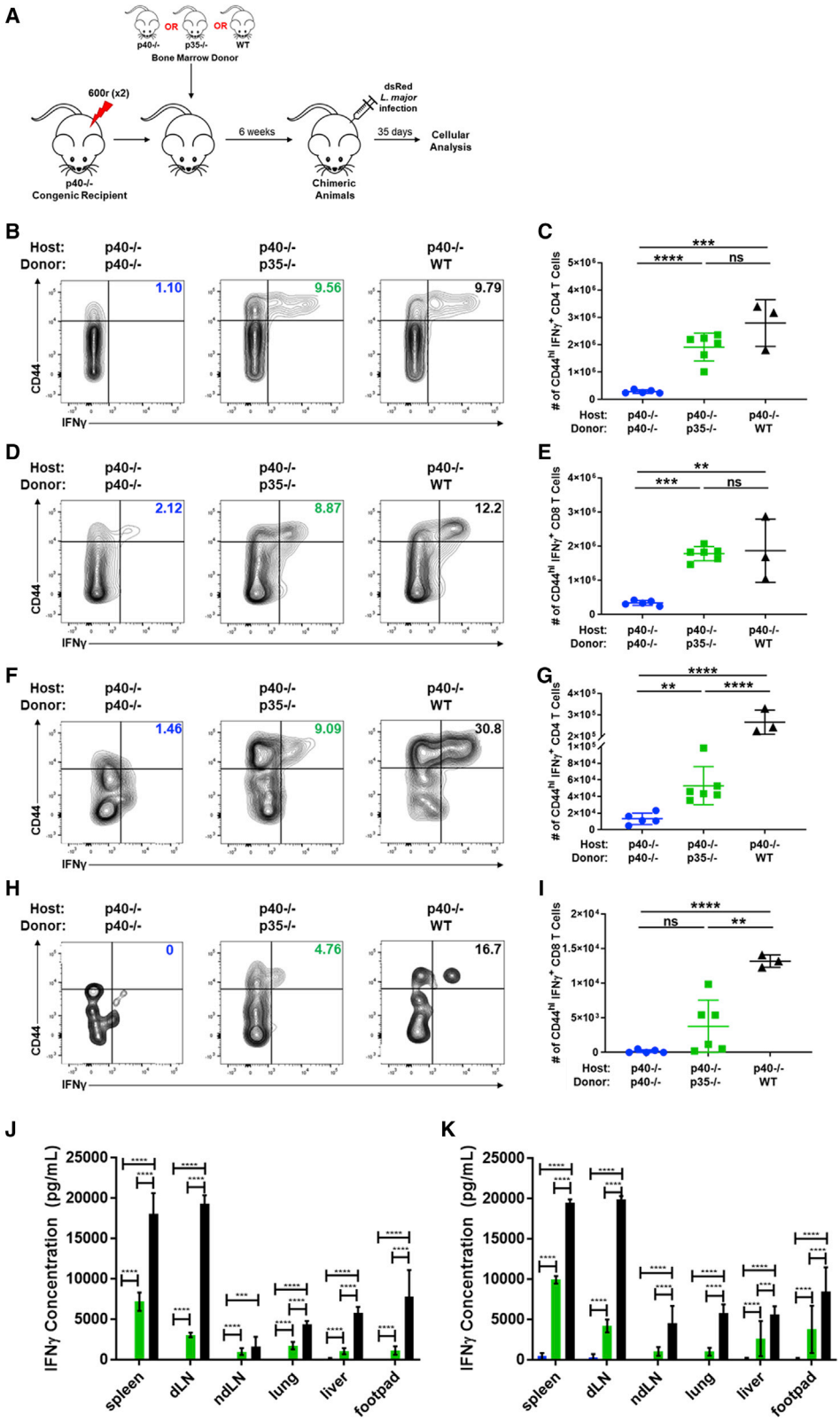

(legend on next page)

chimeras in all tissues analyzed (Figures 4J and 4K). Taken together, these data suggest that two-cell IL-12 can still elicit IFNγ from CD4 T cells at the primary site of infection but to a lower degree than for canonical IL-12.

Hematopoietic expression of p40 is critical for the two-cell IL-12 activity

The separable contribution by two different cells of subunits toward heterodimeric IL-12 assembly raises several key questions, not the least of which is the category of cells involved. Typically, DCs are considered the primary source of both monomeric p40 and heterodimeric IL-12. While p40 is primarily expressed by DCs and macrophages (typically hematopoietic cells), there is evidence that p35 can be sourced from other cells (Figures S5A and S5B). Thus, we examined a chimeric situation where $p35^{-/-}$ hosts (capable of making p40) were irradiated and reconstituted with $p35^{-/-}$, $p40^{-/-}$, or WT bone marrow (Figure 5A).

With lethal split dose irradiation, the hematopoietic compartment is ablated in these mice (Figures S3B and S3C). Therefore, in the $p40^{-/-} \rightarrow p35^{-/-}$ setup, the host cells would be unable to produce p40 for two-cell IL-12 production seen with the $p40^{-/-}$ host chimeras in Figure 3. Thus, only the $WT \rightarrow p35^{-/-}$ animals were able to induce a $CD44^{hi}$ CD4 population of IFNγ-producing cells, similar to levels seen in $WT \rightarrow p40^{-/-}$ chimeras, at 10.9% (±1.8%) (Figures 5B and S5C). Both $p35^{-/-} \rightarrow p35^{-/-}$ and $p40^{-/-} \rightarrow p35^{-/-}$ chimeras had comparable minimal frequencies (Figures 5B and S5C) as well as numbers of $CD44^{hi}$ IFNγ-producing CD4 T cells in the spleen (Figure 5C). Similar trends were also seen in CD8 cells (Figures 5D, 5E, and S5D). Therefore, a hematopoietic cell is the necessary source of p40 production for two cell-derived IL-12 to be made *in vivo*.

Unlike the lethal split dose radiation used above, sublethal irradiation at 600 rad allows for the retention of some hematopoietic cells within host animals (Figures S3B and S3C). Under these conditions, $p35^{-/-}$ chimeras would still retain host-derived cells capable of producing p40. Importantly, T cells in these $p40^{-/-} \rightarrow p35^{-/-}$ chimeric mice produced IFNγ in a comparable proportion to $WT \rightarrow p35^{-/-}$ animals (Figures S5E and S5G). The total number of IFNγ-producing CD4 (Figure S5F) and CD8 (Figure S5H) T cells in the spleen followed the same trends. Comparing these results with the $p40^{-/-} \rightarrow p35^{-/-}$ animals that were subjected to split dose lethal irradiation confirms that the hematopoietic compartment is responsible for the production of p40 in the two-cell model. The cellular source of p35 is not as limiting, as suggested by the expression data (Figure S5B) and previous studies that have found p35 expression in keratinocytes and fibroblast-like cells (Aragane et al., 1994; Carrión et al., 2013). As such, when comparing the single-dose 600r chimeras made with $p40^{-/-}$ hosts, where p35 can be produced by the hematopoietic compartment as well as stromal cells, to the lethal split dose in Figure 4, where it is limited to solely stromal cell production, we find that the induction of IFNγ in the $p35^{-/-} \rightarrow p40^{-/-}$ animals is comparable in both CD4 and CD8 T cells (Figures S5I and S5J). This indicates that p35 is not restricted to the hematopoietic compartment as for p40. Taken together, we infer that bone marrow-derived cells are critical as the source of p40, while p35 can be derived from non-hematopoietic sources for two-cell IL-12 to drive functional IFNγ responses. This agrees with expression data previously published and suggests a localized, tissue expression of p35 while p40, expressed and released by antigen-presenting cells, circulates to form IL-12 wherever p35 is expressed.

The functional significance of two cell- versus one cell-derived IL-12 activity

The chimeric model offered an opportunity to evaluate whether the IFNγ-promoting activity derived from canonical IL-12 versus two-cell IL-12 assembly has differing impacts on the course of the infection. Interestingly, despite the IFNγ production seen from two-cell IL-12 (Figure 4), *L. major* infection, as monitored by swelling of the footpad midpoint, revealed no difference between $p40^{-/-} \rightarrow p40^{-/-}$ and $p35^{-/-} \rightarrow p40^{-/-}$ animals, with

Figure 4. Two-cell formation of IL-12 triggers downstream IFNγ in response to *L. major* infection

(A) Schematic of experimental design. Bone marrow chimeras were generated by reconstituting irradiated $CD45.1^{+}$ $p40^{-/-}$ with bone marrow cells from $CD45.2^{+}$ $p40^{-/-}$, $CD45.2^{+}$ $p35^{-/-}$, or $CD45.1^{+}CD45.2^{+}$ WT donor mice. Chimeric mice were infected in the footpad dermis with 10^6 dsRed *L. major* parasites following reconstitution. 35 days after infection, tissues were harvested and restimulated for intracellular cytokine staining and flow cytometric analysis. Gating strategy used for these panels is shown in Figure S3A.

(B) Percentage and of $CD44^{hi}IFN\gamma^{+}CD4^{+}$ T cells in the spleen of $p40^{-/-}$ host chimeras measured 35 days after infection ($p40^{-/-} \rightarrow p40^{-/-}$, n = 4; $p35^{-/-} \rightarrow p40^{-/-}$, n = 6; $WT \rightarrow p40^{-/-}$, n = 3).

(C) Number of $CD44^{hi}IFN\gamma^{+}CD4^{+}$ T cells in the spleen of $p40^{-/-}$ host chimeras reconstituted with $p40^{-/-}$ (circles, blue), $p35^{-/-}$ (squares, green), or WT (triangles, black) donor bone marrow 35 days after infection (unpaired t test, $p40^{-/-} \rightarrow p40^{-/-}$, n = 4; $p35^{-/-} \rightarrow p40^{-/-}$, n = 6; $WT \rightarrow p40^{-/-}$, n = 3).

(D) Same as in (B), except $CD8^{+}$ T cells ($p40^{-/-} \rightarrow p40^{-/-}$, n = 4; $p35^{-/-} \rightarrow p40^{-/-}$, n = 6; $WT \rightarrow p40^{-/-}$, n = 3).

(E) Same as in (C), except $CD8^{+}$ T cells (unpaired t test, $p40^{-/-} \rightarrow p40^{-/-}$, n = 4; $p35^{-/-} \rightarrow p40^{-/-}$, n = 6; $WT \rightarrow p40^{-/-}$, n = 3).

(F) Percentage of $CD44^{hi}IFN\gamma^{+}CD4^{+}$ T cells in lymphocytes harvested from the footpad lesion tissue of $p40^{-/-}$ host chimeras 35 days after infection ($p40^{-/-} \rightarrow p40^{-/-}$, n = 4; $p35^{-/-} \rightarrow p40^{-/-}$, n = 6; $WT \rightarrow p40^{-/-}$, n = 3).

(G) Number of $CD44^{hi}IFN\gamma^{+}CD4^{+}$ T cells in lymphocytes harvested from the footpad lesion of $p40^{-/-}$ host chimeras reconstituted with $p40^{-/-}$ (circles, blue), $p35^{-/-}$ (squares, green), or WT (triangles, black) donor bone marrow 35 days after infection (unpaired t test, $p40^{-/-} \rightarrow p40^{-/-}$, n = 4; $p35^{-/-} \rightarrow p40^{-/-}$, n = 6; $WT \rightarrow p40^{-/-}$, n = 3).

(H) Same as in (F), except $CD8^{+}$ T cells ($p40^{-/-} \rightarrow p40^{-/-}$, n = 4; $p35^{-/-} \rightarrow p40^{-/-}$, n = 6; $WT \rightarrow p40^{-/-}$, n = 3).

(I) Same as in (G), except $CD8^{+}$ T cells (unpaired t test, $p40^{-/-} \rightarrow p40^{-/-}$, n = 4; $p35^{-/-} \rightarrow p40^{-/-}$, n = 6; $WT \rightarrow p40^{-/-}$, n = 3).

(J and K) Cells from each tissue were harvested 35 days after infection and restimulated with soluble *Leishmania* antigen (SLA). Concentrations are shown of IFNγ in supernatant by tissues collected from $p40^{-/-} \rightarrow p40^{-/-}$ (blue), $p35^{-/-} \rightarrow p40^{-/-}$ (green), and $WT \rightarrow p40^{-/-}$ (black) after restimulation for (J) 24 and (K) 48h (unpaired t test, $p40^{-/-} \rightarrow p40^{-/-}$, n = 4; $p35^{-/-} \rightarrow p40^{-/-}$, n = 6; $WT \rightarrow p40^{-/-}$, n = 3).

Data in this figure are representative of two independent experiments where n refers to the number of biological replicates. (C), (E), (G), and (I)–(K) are displayed as mean ± SEM. *p < 0.05, **p < 0.01, ***p < 0.001, ****p < 0.0001. Anything not marked is considered not statistically significant.

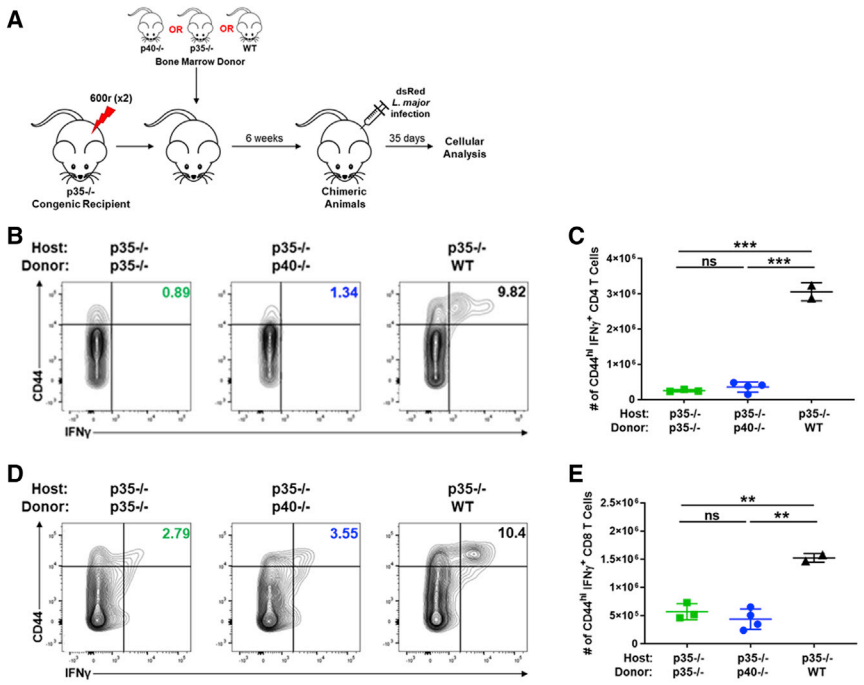

Figure 5. Hematopoietic cell expression of p40 is critical for two-cell IL-12 formation

(A) Schematic of experimental design. Bone marrow chimeras were generated by reconstituting irradiated CD45.2$^+$ p35$^{-/-}$ mice with bone marrow cells from CD45.1$^+$ p40$^{-/-}$, CD45.2$^+$ p35$^{-/-}$, or CD45.1$^+$CD45.2$^+$ WT donor mice. Chimeric mice were infected in the footpad dermis with 10^6 dsRed *L. major* parasites following reconstitution. 35 days after infection, tissues were harvested and restimulated for intracellular cytokine staining and flow cytometric analysis. Gating strategy used for these panels is shown in Figure S3A.

(B) Percentage of CD44^{hi}IFNγ$^+$CD4$^+$ T cells in the spleen of p35$^{-/-}$ host chimeras measured 35 days after infection (p35$^{-/-}$→p35$^{-/-}$, n = 3; p40$^{-/-}$→p35$^{-/-}$, n = 3; WT→p35$^{-/-}$, n = 2).

(C) Number of CD44^{hi}IFNγ$^+$CD4$^+$ T cells in the spleen of p35$^{-/-}$ host chimeras reconstituted with p35$^{-/-}$ (squares, green), p40$^{-/-}$ (circles, blue), or WT (triangles, black) donor bone marrow 35 days after infection (unpaired t test, p35$^{-/-}$→p35$^{-/-}$, n = 3; p40$^{-/-}$→p35$^{-/-}$, n = 3; WT→p35$^{-/-}$, n = 2 due to animal death).

(D) Same as in (B), except CD8$^+$ T cells (p35$^{-/-}$→p35$^{-/-}$, n = 3; p40$^{-/-}$→p35$^{-/-}$, n = 3; WT→p35$^{-/-}$, n = 2).

(E) Same as in (C), except CD8$^+$ T cells (unpaired t test, p35$^{-/-}$→p35$^{-/-}$, n = 3; p40$^{-/-}$→p35$^{-/-}$, n = 3; WT→p35$^{-/-}$, n = 2).

Data in this figure are representative of two independent experiments where n refers to the number of biological replicates. The WT groups in these experiments are limited to n = 2 due to technical reasons; however, combining the 600r chimeras (Figure S5) with the WT groups here allows us to have four groups of WT mice, and they were not significantly different in the two experiments. (C) and (E) are displayed as mean ± SEM. *p < 0.05, **p < 0.01, ***p < 0.001, ****p < 0.0001. Anything not marked is considered not statistically significant.

both developing non-healing lesions while WT→p40$^{-/-}$ animal lesions healed over time, returning to near baseline levels of footpad thickness (Figures 6A and 6B). Consistent with this, initial analysis of parasite numbers at the footpad showed total parasite titers comparably high, near 10^{15} for both p40$^{-/-}$→p40$^{-/-}$ and p35$^{-/-}$→p40$^{-/-}$ animals, while WT→p40$^{-/-}$ total parasite levels were reduced, near 10^8 by the experimental endpoint (Figure 6C).

Although *L. major* is traditionally studied as a localized infection (especially in resistant B6 mice), it is also known to disseminate fairly systemically (Kamala and Nanda, 2009; Kurey et al., 2009; Nicolas et al., 2000; Rossi and Fasel, 2018; Sacks and Noben-Trauth, 2002; Wege et al., 2012). Of particular note, the liver is a known site affected in severe *L. major* infections (Hu et al., 2018). We therefore examined representative tissue sites in the chimeric mice for parasitemia to determine the impact of two-cell IL-12 on parasite control at these sites. Importantly, we used a limiting dilution assay, which only evaluates live replicating parasites rather than genetic material from dead parasites. We validated that disseminating parasites are viable by propidium iodide staining (Figures S6J–S6N).

The data from these assays allowed us to unravel a striking tissue specificity to the biological activity the two-cell IL-12, toward limiting parasite burden in the organs we examined. Unlike the footpad (where the p35$^{-/-}$→p40$^{-/-}$ chimera failed to control parasite burden any better than did the p40$^{-/-}$ mice; Figure 6C), we noticed that the parasite loads in the dLN were already different (Figure 6D). Compared to the WT mice, p40$^{-/-}$→p40$^{-/-}$ had an approximately 2-log higher parasite load. However, unlike the footpad samples, p35$^{-/-}$→p40$^{-/-}$ animals had parasite numbers reduced about 3-fold from those in the p40$^{-/-}$→p40$^{-/-}$ group, although they were still quite higher than those in the WT→p40$^{-/-}$ group. In striking contrast, when we enumerated parasite count at a distal non-dLN (ndLN) (Figure 6E), the parasite load between the p35$^{-/-}$→p40$^{-/-}$ chimeras and the WT→p40$^{-/-}$ was not statistically distinguishable, suggesting that both groups control dissemination to this distant site, much better than the p40$^{-/-}$→p40$^{-/-}$ chimeric mice. Furthermore, evaluation of additional tissue sites (spleen, liver, and lung in Figures 6F–6H) showed a range of differences, with the p35$^{-/-}$→p40$^{-/-}$ chimeras consistently controlling parasite burden better that the p40$^{-/-}$→p40$^{-/-}$ chimeras in each case. As shown in Figure 5, chimeras set up with p35$^{-/-}$ host animals are unable to form two-cell IL-12, as the hematopoietic source of p40 is ablated with irradiation in these animals. Thus, both the p35$^{-/-}$→p35$^{-/-}$ and p40$^{-/-}$→p35$^{-/-}$ animals have similar parasite titers in all tissues analyzed, confirming the absence of two-cell IL-12 and its role in limiting the dissemination of parasites (Figures S6A–S6H).

Taken together, these data demonstrate a gradation of the impact of two-cell IL-12 activity depending on the tissue type. The primary site of infection and the nearby dLN sites need the canonical one-cell production of IL-12 to clear the parasite. Distant sites, such as the spleen, liver, lung, and ndLNs, can impart significant infection control with solely two-cell production of IL-12.

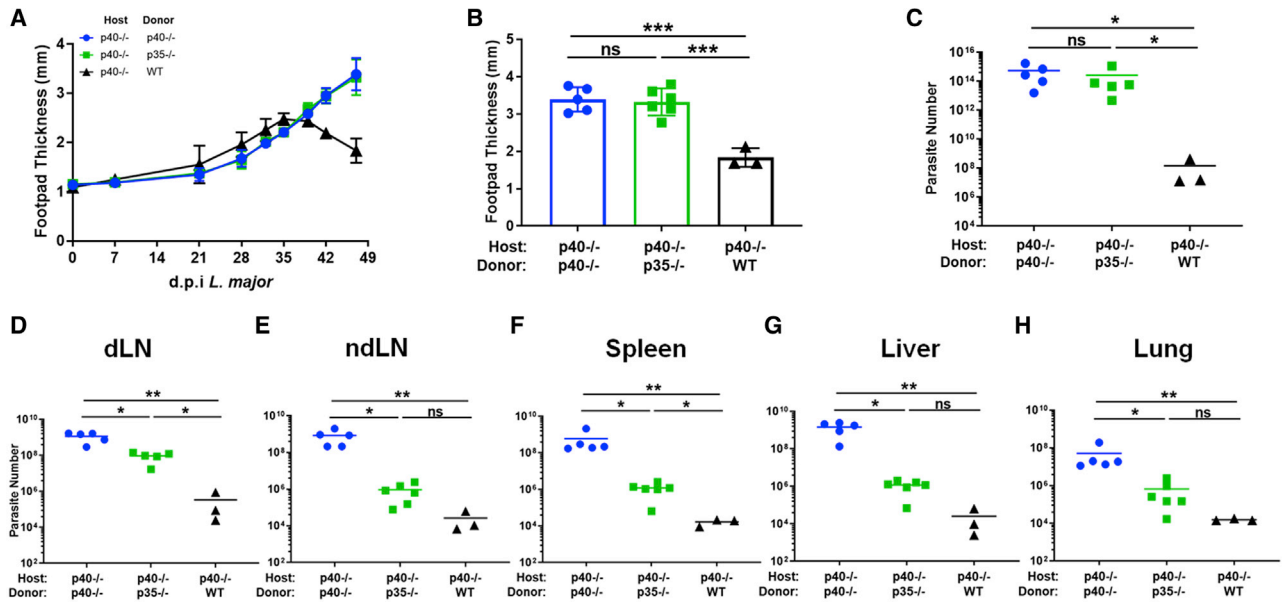

Figure 6. Two cell-derived IL-12 activity is functionally different than one-cell derived IL-12 activity

Bone marrow chimeras were generated by reconstituting irradiated CD45.1$^+$ p40$^{-/-}$ mice with bone marrow cells from CD45.2$^+$ p40$^{-/-}$, CD45.2$^+$ p35$^{-/-}$, or CD45.1$^+$CD45.2$^+$ WT donor mice. Chimeric mice were infected in the footpad dermis with 10^6 dsRed *L. major* parasites following reconstitution.

(A) Biweekly measurement of footpad thickness at the midline following establishment of visible lesion for p40$^{-/-}$ host chimeras reconstituted with p40$^{-/-}$ (circles, blue), p35$^{-/-}$ (squares, green), or WT (triangles, black) through the duration of infection (p40$^{-/-}$ → p40$^{-/-}$, n = 4; p35$^{-/-}$ → p40$^{-/-}$, n = 6; WT → p40$^{-/-}$, n = 3).

(B) Footpad thickness at the midline of p40$^{-/-}$ host chimeras reconstituted with p40$^{-/-}$ (circles, blue), p35$^{-/-}$ (squares, green), or WT (triangles, black) 35 days after *L. major* infection (unpaired t test, p40$^{-/-}$ → p40$^{-/-}$, n = 4; p35$^{-/-}$ → p40$^{-/-}$, n = 6; WT → p40$^{-/-}$, n = 3).

(C–H) dsRed *L. major* parasite quantified by limiting dilution from (C) footpad lesion, (D) dLN, (E) non-dLN (ndLN), (F) spleen, (G) liver, and (H) lung tissue of p40$^{-/-}$ host chimeras reconstituted with p40$^{-/-}$ (circles, blue), p35$^{-/-}$ (squares, green), or WT (triangles, black) 35 days after infection (unpaired t test, p40$^{-/-}$ → p40$^{-/-}$, n = 4; p35$^{-/-}$ → p40$^{-/-}$, n = 6; WT → p40$^{-/-}$, n = 3).

Data in this figure are representative of two independent experiments where n refers to the number of biological replicates. All data are displayed as mean ± SEM. *p < 0.05, **p < 0.01, ***p < 0.001, ****p < 0.0001. Anything not marked is considered not statistically significant.

DISCUSSION

Data presented herein demonstrate using multiple experimental approaches that functional IL-12 can be formed through the collaborative production of individual subunits by two separate cells: p40 from hematopoietic cells and p35 from other cells. Importantly, the chimeric approach also allows us to evaluate the functional significance of this form of IL-12 during protective immune responses to a pathogen, as modeled by *L. major.* The structural ability of p40 to bind p35 has been extensively characterized, although focusing on assembly within a single cell (Glassman et al., 2021; Lupardus and Garcia, 2008; Yoon et al., 2000). In the present study, we extend previous work (mostly using *in vitro* models) suggesting that the two proteins can also functionally assemble outside the cell. This functional assembly is consistent with previous literature and gene expression datasets showing that p40 expression is limited to DCs and macrophages (D'Andrea et al., 1992) while p35 expression is more widespread (Dixon et al., 2015; Sha et al., 2015; Shen et al., 2014). In the past decade, the contribution of non-hematopoietic cells toward modulating the trajectory of an immune response has been extensively discussed (Matzinger and Kamala, 2011). The mechanism of IL-12 assembly we demonstrate herein adds an important dimension to this emerging picture, suggesting that heterodimeric cytokines may possess an intrinsic advantage by allowing their subunits to not only reassort to form multiple cytokines, but also source the subunits from different tissues. This has the potential to molecularly encode immunological context, with both sentinel cells (e.g., DCs, macrophages) and stromal cells collaborating to jointly shape the trajectory of T cell differentiation (Abdi and Singh, 2015). Importantly, note that while the data demonstrate that two separate cells can contribute parts of IL-12 *in vivo*, the significance of the specific source of p35 needs to be resolved further. Importantly, in chimeras where we used WT bone marrow to reconstitute either p40$^{-/-}$ (WT groups in Figures 4B and 4D) or p35$^{-/-}$ (WT groups in Figures 5B and 5D), there was no significant differences in T cell differentiation, suggesting that at least for that parameter, the availability of p40 and p35 from hematopoietic cells was redundant with stromal cells. Intriguingly, we found that the levels of IL-10 secretion by WT T cells developing in a p35$^{-/-}$ stromal environment were significantly (~3.5-fold) greater than those in the p35-sufficient but p40$^{-/-}$ stroma (Figure S5L). Certainly, IL-10 is part of the negative feedback loop elicited by IFNγ and IL-12 (Abdi et al., 2012; D'Andrea et al., 1993); however, how stromal p35 selectively impacts that is not immediately clear and will require additional studies.

If such studies are also extended to additional cytokines such as IL-23, it is possible that a major driver of IFNγ versus IL-17 differentiation in some cases may be the expression of p35 versus p19 by specific stromal cells, rather than DCs themselves. In the chimeric models, although we did notice a trend toward higher IL-17 production in the $p35^{-/-}$ chimeric mice (Figures S4F and S4G), this was not statistically significant. Importantly, the IL-4 production that is associated with IL-12 deficiency was also corrected in the chimeric mice (Figures S4H and S4I). This suggests that the two-cell form of IL-12 can recapitulate most known activities of canonical IL-12.

Nevertheless, two-cell IL-12 does not appear to be sufficient to control *L. major* at the primary infection site. This is an intriguing observation and illustrates key aspects by which localized immunity in secondary sites can differ from the primary site of infection. For one, the failure to control parasites at the primary site while having robust control at specific distal sites was not correlated with differences in T cell differentiation toward IFNγ production. While there is an extensive literature suggesting that the IL-12/IFNγ axis is critical for the control of *Leishmania*, the direct evidence in our study is limited to showing that two-cell IL-12 regulates IFNγ and also dissemination. Future experiments will have to evaluate (using IFNγ double knockouts with p40 and p35) whether the IFNγ is causal for limiting tissue dissemination. If it is, one possible explanation for the dichotomy in the functional roles of two-cell versus one-cell IL-12 is that they reflect kinetic variations in the amount of IL-12: while both early and late IL-12 production could be sufficient to drive T cell differentiation, perhaps sustained production is required for control at each site. This is challenging to measure dynamically. For one, the amount of two-cell IL-12 formed *in vivo* was not detectable using commercial ELISAs (Figure S4J). Yet, clearly, by multiple readouts there is sufficient *in vivo* availability to drive T cell differentiation. An alternate possibility is that the two-cell form is nucleated by cell-specific process, akin to the trans-presentation of IL-15 (and therefore difficult to detect in circulation).

Canonical IL-12 is formed when p40 disulfide bonds with p35, allowing for both subunits to be secreted. Yet, this covalent association has been shown to be dispensable for secretion of the functional IL-12 cytokine (Reitberger et al., 2017; Yoon et al., 2000). Furthermore, this is not the only route to p35 release, as p35 binds to another known partner (Ebi3) to form IL-35, after these subunits are reportedly released independently (Aparicio-Siegmund et al., 2014; Sawant et al., 2015). We had previously shown that functional IL-12 can be generated *in vitro* through the collaborative combination of either p40 monomer with p35 released from necrotic cells or the reverse combination of p35 with p40 from serum (Abdi et al., 2014). Thus, mechanistically, the release of p35 *in vivo* can also be through necrotic cell death upon tissue damage by a pathogen. This would infer that the innate immune system is integrating two signals in informing T cells about the desired route of differentiation (Abdi and Singh, 2015). First, engagement of PRRs on DCs would lead to p40 release, which disseminates systemically albeit in an inert form (does not drive T cell differentiation). Second, the arrival of pathogen in specific tissue sites allows for local and appropriate release of p35. According to this model, distinct tissue sites can control the quantity of the effector response by regulating p35 release and perhaps even the quality by releasing p19 versus p35. A third possibility is in tissue-specific variations in the induction of IFNγ itself. Multiple cytokines (including IL-18 and IL-15) as well as T cell-derived signals (via CD40) can influence the ability of cells to make IFNγ (Abdi et al., 2006; Abdi and Singh, 2010) (Denton et al., 2007; Müller et al., 2001). In many cases, IL-12 is more associated with a feedback loop for amplification of IFNγ production rather than the initial triggering. Tissue levels of such triggers or other negative regulators (transforming growth factor β [TGF]-β, IL-10) can potentially contribute to these differences as well.

L. major infects multiple cell types although often studied as a localized infection. Previous reports, especially in susceptible strains of mice, have shown that the parasite can travel via infected cells to multiple tissues (Kurey et al., 2009; Nicolas et al., 2000; Rossi and Fasel, 2018; Sacks and Noben-Trauth, 2002; Wege et al., 2012). Dissemination of the *L. major* parasite has been shown to be aided by inflammatory DCs infected with the parasite (Hurdayal et al., 2013, 2020). In addition, *L. major* is known to downregulate transcription of both p40 and p35 subunits in macrophages and monocytes (Belkaid et al., 1998; Sartori et al., 1997). Taking this into account, production of p35 at disseminated tissue sites would contribute to a greater IL-12 response necessary for local parasite control. The presence of elevated p40 levels detected in the serum allow for the circulation among secondary infection sites and subsequent binding to p35 for the formation of two-cell IL-12. A reviewer of this manuscript suggested that this could perhaps relate to vascularization of each organ and the kinetics of p40 "arrival" or accumulation there. This intriguing hypothesis remains to be tested. In this context, the experiments with recombinant administration of p40 (Figure 2) can be a useful approach.

Collectively, the data we have shown herein establishes that IL-12 activity can come from the collaboration between two distinct cells and impact T cell differentiation to IFNγ production. The functional, *in vivo* demonstration of the two-cell mechanism of IL-12 assembly allows for consideration of both mechanisms in other disease states as well as potentially understanding clinical conditions where distinct pools of systemic and local IL-12 can have different consequences.

STAR★METHODS

Detailed methods are provided in the online version of this paper and include the following:

- KEY RESOURCES TABLE
- RESOURCE AVAILABILITY
  - Lead contact
  - Materials availability
  - Data and code availability
- EXPERIMENTAL MODEL AND SUBJECT DETAILS
  - Mice
  - Parasite lines
- METHOD DETAILS
  - Generation of bone marrow chimeras
  - Preparation of soluble *Leishmania* antigen

- *Leishmania* infection of animals
- Adoptive transfer and antigen challenge
- Tissue preparation
- Intracellular stain and flow cytometry analysis
- Parasite quantification
- Live parasite analysis by flow cytometry
- Cytokine production quantification

● QUANTIFICATION AND STATISTICAL ANALYSIS

SUPPLEMENTAL INFORMATION

Supplemental information can be found online at https://doi.org/10.1016/j.celrep.2021.109816.

ACKNOWLEDGMENTS

We thank members of the Nevil laboratory—Courtney Matson, Kenneth Rosenberg, Gideon Wolf, and Zachary Fasana—for assistance with mouse takedowns, discussions, and critiques during the development of this work; Dr. David L. Sacks for the dsRed-*L. major* parasites; Drs. Yasmine Belkaid and Alain Debrabant for assistance setting up *L. major* protocols; and the University of Maryland Greenebaum Comprehensive Cancer Center Flow Cytometry Core and Dr. Xiaoxuan Fan for flow cytometry support. This work was supported by NIH grants R01 AI110719, R21 AI149076, and R21 AI166330 (to N.J.S.).

AUTHOR CONTRIBUTIONS

A.N.G. conceived experiments, performed all experiments, analyzed the data, prepared figures, and wrote the paper. K.A. conceived the experimental plan and participated in data analysis and editing paper. N.J.S. conceived experiments, secured funding, performed experiments, analyzed data, supervised the project, and wrote the paper.

DECLARATION OF INTERESTS

The authors declare no competing interests.

Received: October 19, 2020
Revised: May 4, 2021
Accepted: September 20, 2021
Published: October 12, 2021

REFERENCES

Abdi, K., and Singh, N.J. (2010). Antigen-activated T cells induce IL-12p75 production from dendritic cells in an IFN-γ-independent manner. Scand. J. Immunol. *72*, 511–521.

Abdi, K., and Singh, N.J. (2015). Making many from few: IL-12p40 as a model for the combinatorial assembly of heterodimeric cytokines. Cytokine *76*, 53–57.

Abdi, K., Singh, N., and Matzinger, P. (2006). T-cell control of IL-12p75 production. Scand. J. Immunol. *64*, 83–92.

Abdi, K., Singh, N.J., and Matzinger, P. (2012). Lipopolysaccharide-activated dendritic cells: "Exhausted" or alert and waiting? J. Immunol. *188*, 5981–5989.

Abdi, K., Singh, N.J., Spooner, E., Kessler, B.M., Radaev, S., Lantz, L., Xiao, T.S., Matzinger, P., Sun, P.D., and Ploegh, H.L. (2014). Free IL-12p40 monomer is a polyfunctional adapter for generating novel IL-12-like heterodimers extracellularly. J. Immunol. *192*, 6028–6038.

Afonso, L.C., Scharton, T.M., Vieira, L.Q., Wysocka, M., Trinchieri, G., and Scott, P. (1994). The adjuvant effect of interleukin-12 in a vaccine against *Leishmania major*. Science *263*, 235–237.

Aparicio-Siegmund, S., Moll, J.M., Lokau, J., Grusdat, M., Schröder, J., Plöhn, S., Rose-John, S., Grötzinger, J., Lang, P.A., Scheller, J., and Garbers, C. (2014). Recombinant p35 from bacteria can form interleukin (IL-)12, but not IL-35. PLoS ONE *9*, e107990.

Aragane, Y., Riemann, H., Bhardwaj, R.S., Schwarz, A., Sawada, Y., Yamada, H., Luger, T.A., Kubin, M., Trinchieri, G., and Schwarz, T. (1994). IL-12 is expressed and released by human keratinocytes and epidermoid carcinoma cell lines. J. Immunol. *153*, 5366–5372.

Belkaid, Y., Butcher, B., and Sacks, D.L. (1998). Analysis of cytokine production by inflammatory mouse macrophages at the single-cell level: Selective impairment of IL-12 induction in Leishmania-infected cells. Eur. J. Immunol. *28*, 1389–1400.

Carra, G., Gerosa, F., and Trinchieri, G. (2000). Biosynthesis and posttranslational regulation of human IL-12. J. Immunol. *164*, 4752–4761.

Carrión, M., Pérez-García, S., Jimeno, R., Juarranz, Y., González-Álvaro, I., Pablos, J.L., Gutiérrez-Cañas, I., and Gomariz, R.P. (2013). Inflammatory mediators alter interleukin-17 receptor, interleukin-12 and -23 expression in human osteoarthritic and rheumatoid arthritis synovial fibroblasts: Immunomodulation by vasoactive intestinal peptide. Neuroimmunomodulation *20*, 274–284.

Cooper, A.M., and Khader, S.A. (2007). IL-12p40: An inherently agonistic cytokine. Trends Immunol. *28*, 33–38.

D'Andrea, A., Rengaraju, M., Valiante, N.M., Chehimi, J., Kubin, M., Aste, M., Chan, S.H., Kobayashi, M., Young, D., Nickbarg, E., et al. (1992). Production of natural killer cell stimulatory factor (interleukin 12) by peripheral blood mononuclear cells. J. Exp. Med. *176*, 1387–1398.

D'Andrea, A., Aste-Amezaga, M., Valiante, N.M., Ma, X., Kubin, M., and Trinchieri, G. (1993). Interleukin 10 (IL-10) inhibits human lymphocyte interferon gamma-production by suppressing natural killer cell stimulatory factor/IL-12 synthesis in accessory cells. J. Exp. Med. *178*, 1041–1048.

Denton, A.E., Doherty, P.C., Turner, S.J., and La Gruta, N.L. (2007). IL-18, but not IL-12, is required for optimal cytokine production by influenza virus-specific $CD8^+$ T cells. Eur. J. Immunol. *37*, 368–375.

Dixon, K.O., van der Kooij, S.W., Vignali, D.A., and van Kooten, C. (2015). Human tolerogenic dendritic cells produce IL-35 in the absence of other IL-12 family members. Eur. J. Immunol. *45*, 1736–1747.

Fowell, D.J., and Locksley, R.M. (1999). *Leishmania major* infection of inbred mice: Unmasking genetic determinants of infectious diseases. BioEssays *21*, 510–518.

Glassman, C.R., Mathiharan, Y.K., Jude, K.M., Su, L., Panova, O., Lupardus, P.J., Spangler, J.B., Ely, L.K., Thomas, C., Skiniotis, G., and Garcia, K.C. (2021). Structural basis for IL-12 and IL-23 receptor sharing reveals a gateway for shaping actions on T versus NK cells. Cell *184*, 983–999.e24.

Gubler, U., Chua, A.O., Schoenhaut, D.S., Dwyer, C.M., McComas, W., Motyka, R., Nabavi, N., Wolitzky, A.G., Quinn, P.M., Familletti, P.C., et al. (1991). Coexpression of two distinct genes is required to generate secreted bioactive cytotoxic lymphocyte maturation factor. Proc. Natl. Acad. Sci. USA *88*, 4143–4147.

Hayes, M.P., Wang, J., and Norcross, M.A. (1995). Regulation of interleukin-12 expression in human monocytes: Selective priming by interferon-γ of lipopolysaccharide-inducible p35 and p40 genes. Blood *86*, 646–650.

Heinzel, F.P., Sadick, M.D., Holaday, B.J., Coffman, R.L., and Locksley, R.M. (1989). Reciprocal expression of interferon gamma or interleukin 4 during the resolution or progression of murine leishmaniasis. Evidence for expansion of distinct helper T cell subsets. J. Exp. Med. *169*, 59–72.

Hu, S., Marshall, C., Darby, J., Wei, W., Lyons, A.B., and Körner, H. (2018). Absence of tumor necrosis factor supports alternative activation of macrophages in the liver after infection with *Leishmania major*. Front. Immunol. *9*, 1.

Hurdayal, R., Nieuwenhuizen, N.E., Revaz-Breton, M., Smith, L., Hoving, J.C., Parihar, S.P., Reizis, B., and Brombacher, F. (2013). Deletion of IL-4 receptor alpha on dendritic cells renders BALB/c mice hypersusceptible to Leishmania major infection. PLoS Pathog. *9*, e1003699.

Hurdayal, R., Nieuwenhuizen, N.E., Khutlang, R., and Brombacher, F. (2020). Inflammatory dendritic cells, regulated by IL-4 receptor alpha signaling,

control replication, and dissemination of *Leishmania major* in mice. Front. Cell. Infect. Microbiol. *9*, 479.

Jalah, R., Rosati, M., Ganneru, B., Pilkington, G.R., Valentin, A., Kulkarni, V., Bergamaschi, C., Chowdhury, B., Zhang, G.M., Beach, R.K., et al. (2013). The p40 subunit of interleukin (IL)-12 promotes stabilization and export of the p35 subunit: Implications for improved IL-12 cytokine production. J. Biol. Chem. *288*, 6763–6776.

Kamala, T., and Nanda, N.K. (2009). Protective response to *Leishmania major* in BALB/c mice requires antigen processing in the absence of DM. J. Immunol. *182*, 4882–4890.

Kimblin, N., Peters, N., Debrabant, A., Secundino, N., Egen, J., Lawyer, P., Fay, M.P., Kamhawi, S., and Sacks, D. (2008). Quantification of the infectious dose of *Leishmania major* transmitted to the skin by single sand flies. Proc. Natl. Acad. Sci. USA *105*, 10125–10130.

Koutoulaki, A., Langley, M., Sloan, A.J., Aeschlimann, D., and Wei, X.Q. (2010). TNFα and TGF-β1 influence IL-18-induced IFNγ production through regulation of IL-18 receptor and T-bet expression. Cytokine *49*, 177–184.

Kurey, I., Kobets, T., Havelková, H., Slapnicková, M., Quan, L., Trtková, K., Grekov, I., Svobodová, M., Stassen, A.P., Hutson, A., et al. (2009). Distinct genetic control of parasite elimination, dissemination, and disease after *Leishmania major* infection. Immunogenetics *61*, 619–633.

Liu, J., Cao, S., Herman, L.M., and Ma, X. (2003). Differential regulation of interleukin (IL)-12 p35 and p40 gene expression and interferon (IFN)-γ-primed IL-12 production by IFN regulatory factor 1. J. Exp. Med. *198*, 1265–1276.

Lupardus, P.J., and Garcia, K.C. (2008). The structure of interleukin-23 reveals the molecular basis of p40 subunit sharing with interleukin-12. J. Mol. Biol. *382*, 931–941.

Matson, C.A., and Singh, N.J. (2020). Manipulating the TCR signaling network for cellular immunotherapy: Challenges & opportunities. Mol. Immunol. *123*, 64–73.

Matzinger, P., and Kamala, T. (2011). Tissue-based class control: The other side of tolerance. Nat. Rev. Immunol. *11*, 221–230.

Müller, U., Köhler, G., Mossmann, H., Schaub, G.A., Alber, G., Di Santo, J.P., Brombacher, F., and Hölscher, C. (2001). IL-12-independent IFN-γ production by T cells in experimental Chagas' disease is mediated by IL-18. J. Immunol. *167*, 3346–3353.

Nicolas, L., Sidjanski, S., Colle, J.H., and Milon, G. (2000). *Leishmania major* reaches distant cutaneous sites where it persists transiently while persisting durably in the primary dermal site and its draining lymph node: A study with laboratory mice. Infect. Immun. *68*, 6561–6566.

Oppmann, B., Lesley, R., Blom, B., Timans, J.C., Xu, Y., Hunte, B., Vega, F., Yu, N., Wang, J., Singh, K., et al. (2000). Novel p19 protein engages IL-12p40 to form a cytokine, IL-23, with biological activities similar as well as distinct from IL-12. Immunity *13*, 715–725.

Park, A.Y., Hondowicz, B.D., and Scott, P. (2000). IL-12 is required to maintain a Th1 response during *Leishmania major* infection. J. Immunol. *165*, 896–902.

Reitberger, S., Haimerl, P., Aschenbrenner, I., Esser-von Bieren, J., and Feige, M.J. (2017). Assembly-induced folding regulates interleukin 12 biogenesis and secretion. J. Biol. Chem. *292*, 8073–8081.

Rossi, M., and Fasel, N. (2018). How to master the host immune system? *Leishmania* parasites have the solutions!. Int. Immunol. *30*, 103–111.

Sacks, D., and Noben-Trauth, N. (2002). The immunology of susceptibility and resistance to *Leishmania major* in mice. Nat. Rev. Immunol. *2*, 845–858.

Sartori, A., Oliveira, M.A., Scott, P., and Trinchieri, G. (1997). Metacyclogenesis modulates the ability of Leishmania promastigotes to induce IL-12 production in human mononuclear cells. J. Immunol. *159*, 2849–2857.

Sawant, D.V., Hamilton, K., and Vignali, D.A. (2015). Interleukin-35: Expanding its job profile. J. Interferon Cytokine Res. *35*, 499–512.

Scott, P., Natovitz, P., Coffman, R.L., Pearce, E., and Sher, A. (1988). Immunoregulation of cutaneous leishmaniasis. T cell lines that transfer protective immunity or exacerbation belong to different T helper subsets and respond to distinct parasite antigens. J. Exp. Med. *168*, 1675–1684.

Sha, X., Meng, S., Li, X., Xi, H., Maddaloni, M., Pascual, D.W., Shan, H., Jiang, X., Wang, H., and Yang, X.F. (2015). Interleukin-35 inhibits endothelial cell activation by suppressing MAPK-AP-1 pathway. J. Biol. Chem. *290*, 19307–19318.

Shen, P., Roch, T., Lampropoulou, V., O'Connor, R.A., Stervbo, U., Hilgenberg, E., Ries, S., Dang, V.D., Jaimes, Y., Daridon, C., et al. (2014). IL-35-producing B cells are critical regulators of immunity during autoimmune and infectious diseases. Nature *507*, 366–370.

Sieburth, D., Jabs, E.W., Warrington, J.A., Li, X., Lasota, J., LaForgia, S., Kelleher, K., Huebner, K., Wasmuth, J.J., and Wolf, S.F. (1992). Assignment of genes encoding a unique cytokine (IL12) composed of two unrelated subunits to chromosomes 3 and 5. Genomics *14*, 59–62.

Sypek, J.P., Chung, C.L., Mayor, S.E., Subramanyam, J.M., Goldman, S.J., Sieburth, D.S., Wolf, S.F., and Schaub, R.G. (1993). Resolution of cutaneous leishmaniasis: Interleukin 12 initiates a protective T helper type 1 immune response. J. Exp. Med. *177*, 1797–1802.

Tait Wojno, E.D., Hunter, C.A., and Stumhofer, J.S. (2019). The immunobiology of the interleukin-12 family: Room for discovery. Immunity *50*, 851–870.

Trinchieri, G. (2003). Interleukin-12 and the regulation of innate resistance and adaptive immunity. Nat. Rev. Immunol. *3*, 133–146.

Tubo, N.J., and Jenkins, M.K. (2014). TCR signal quantity and quality in $CD4^+$ T cell differentiation. Trends Immunol. *35*, 591–596.

Wege, A.K., Florian, C., Ernst, W., Zimara, N., Schleicher, U., Hanses, F., Schmid, M., and Ritter, U. (2012). *Leishmania major* infection in humanized mice induces systemic infection and provokes a nonprotective human immune response. PLoS Negl. Trop. Dis. *6*, e1741.

Yoon, C., Johnston, S.C., Tang, J., Stahl, M., Tobin, J.F., and Somers, W.S. (2000). Charged residues dominate a unique interlocking topography in the heterodimeric cytokine interleukin-12. EMBO J. *19*, 3530–3541.

STAR★METHODS

KEY RESOURCES TABLE

REAGENT or RESOURCE	SOURCE	IDENTIFIER
Antibodies		
Brilliant Violet 605 anti-mouse CD4 clone GK1.5	Biolegend	Cat# 300555; RRID:AB_2564390
eFluor 450 anti-mouse CD4 clone GK1.5	eBioscience	Cat# 48-0041-82; RRID:AB_10718983
Brilliant Violet 650 anti-mouse CD8b clone H35-17.2	BD Biosciences	Cat# 740552; RRID:AB_2740253
FITC anti mouse CD8b clone H35-17.2	eBioscience	Cat# 11-0080-85; RRID:AB_657775
PE/Cyanine7 anti-mouse/human CD11b clone M1/70	Biolegend	Cat# 100215; RRID:AB_312798
eFluor 450 anti-mouse CD11c clone N418	eBioscience	Cat# 48-0114-80; RRID:AB_1548665
PE anti-mouse/human CD44 clone IM7	BD PharMingen	Cat# 553134; RRID:AB_394649
PE-Cy7 anti-mouse/hman CD44 clone IM7	Biolegend	Cat# 103030; RRID:AB_830787
PerCP/Cyanine5.5 anti-mouse/human CD44 clone IM7	Biolegend	Cat# 103032; RRID:AB_2076204
Alexa Fluor 488 anti-mouse CD45.1 clone A20	Biolegend	Cat# 110718; RRID:AB_492862
APC anti-mouse CD45.2 clone 104	eBioscience	Cat# 17-0454-82; RRID:AB_469400
Alexa Fluor 700 anti-mouse CD62L clone MEL-14	Biolegend	Cat# 104426; RRID:AB_493719
PE/Cyanine7 anti-mouse CD62L clone MEL-14	Biolegend	Cat# 104417; RRID:AB_313102
APC anti-mouse IFNγ clone XMG1.2	eBioscience	Cat# 17-7311-82; RRID:AB_469504
FITC anti-mouse IFNγ clone XMG1.2	BD PharMingen	Cat# 554411; RRID:AB_395375
PE anti-mouse IL-4 clone 11B11	Biolegend	Cat# 504104; RRID:AB_315318
PerCP/Cyanine5.5 anti-mouse IL-10 clone JES5-16E3	Biolegend	Cat# 505028; RRID:AB_2561523
APC anti-mouse IL-17A clone TC11-18H10.1	Biolegend	Cat# 506916; RRID:AB_536018
PE anti-mouse MHC Class II (IA/IE) clone M5/114.15.2	eBioscience	Cat# 12-5321-82; RRID:AB_465928
Brilliant Violet 421 anti-mouse T-bet clone 4B10	Biolegend	Cat# 644815; RRID:AB_10896427
PE-Cy7 anti-mouse T-bet clone 4B10	eBioscience	Cat# 12-5825-82; RRID:AB_925761
Brilliant Violet510 anti-mouse TCRβ clone H57-597	Biolegend	Cat# 109233; RRID:AB_2562349
CyChrome anti-mouse TCRβ clone H57-597	BD PharMingen	Cat# 553173; RRID:AB_394685
PE anti-mouse TCR-vβ8.3 clone 1B3.3	BD PharMingen	Cat# 553664; RRID:AB_394980
Biotin anti-mouse NK1.1 clone PK136	eBioscience	Cat# 13-5941-82; RRID:AB_466804
Biotin anti-mouse CD11c clone N418	eBioscience	Cat# 13-0114-82; RRID:AB_466363
Biotin anti-mouse CD8a clone 53-6.7	eBioscience	Cat# 13-0081-82; RRID:AB_466346
Biotin anti-mouse MHC class II clone M5/114.15.2	eBioscience	Cat# 13-5321-82; RRID:AB_466662
Purified anti-mouse CD16/CD32 clone 2.4G2	BD PharMingen	Cat# 553141; RRID:AB_394656
Chemicals, peptides, and recombinant proteins		
LCMV GP_{61-80}	AnaSpec	Cat# AS-64851
Collagenase D	Roche	Cat# 11 088 858 011
Propidium Iodide Solution	Sigma-Aldrich	Cat# P4864
Lipopolysaccharides from *E. coli*	Sigma-Aldrich	Cat# L2880
Medium 199	GIBCO	Cat# 12350039
RPMI 1640	GIBCO	Cat# 11875119
Foundation Fetal Bovine Serum	Gemini Bio	Cat# 900-108
HEPES	GIBCO	Cat# 15-630-080
Adenine	Sigma-Aldrich	Cat# A2786

(*Continued on next page*)

Continued

REAGENT or RESOURCE	SOURCE	IDENTIFIER
Biotin	Sigma-Aldrich	Cat# B4501
Hemin	Sigma-Aldrich	Cat# 51280
PBS	Quality Biological	Cat# 119-069-101
Ficoll Paque Plus	GE Healthcare	Cat# 17-1440-02
Lectin from *Arachis hypogaea* (peanut)	Sigma-Aldrich	Cat# L6135
Sodium Pyruvate	GIBCO	Cat# 11360070
Antibiotic-antimycotic	GIBCO	Cat# 15240062
2-Mercaptoethanol	Sigma-Aldrich	Cat# M6250
Brefeldin A	eBioscience	Cat# 00-4506-51
EDTA	Quality Biological	Cat# 351-027-101
Sodium azide	Sigma-Aldrich	Cat# S2002
Phorbol 12-myristate 13-acetate	Sigma-Aldrich	Cat# P8139
Ionomycin calcium salt	Sigma-Aldrich	Cat# I0634
Triethanolamine	Sigma-Aldrich	Cat# 90278
Critical commercial assays		
Mouse IL-17A (homodimer) ELISA Ready-SET-Go!	eBioscience	Cat# 88-7371 RRID:AB_2575104
Mouse IFN gamma ELISA Ready-SET-Go!	eBioscience	Cat# 88-7314 RRID:AB_2575069
Mouse IL-2 Quantikine ELISA Kit	R&D Systems	Cat# M2000
Mouse IL-4 Quantikine ELISA Kit	R&D Systems	Cat# M4000B
Mouse IL-12 p40 Quantikine ELISA Kit	R&D Systems	Cat# M1240
Mouse IL-12 p70 Quantikine ELISA Kit	R&D systems	Cat# M1270
Dynabeads M-280 Streptavidin	Invitrogen	Cat# 11205D
Cytofix/Cytoperm	BD Biosciences	Cat# 554722
Foxp3 / Transcription Factor Staining Buffer Set	eBioscience	Cat# 00-5523-00
LIVE/DEAD Fixable Near-IR	Invitrogen	Cat# L10119
Ghost Dye Red 780	Tonbo Biosciences	Cat# 13-0865
BCA Protein Assay Kit	Pierce	Cat# 23225
Deposited data		
GTEx Analysis Release V8 (dbGaP Accession phs000424.v8.p2)	GTEx	https://www.gtexportal.org/home/gene/IL12B
Experimental models: Organisms/strains		
L. major-RFP	Kimblin et al., 2008	Kimblin et al., 2008
Mouse: B6.129S1-Il12b^{tm1Jm}/J	The Jackson Laboratory	Cat# 002693
Mouse: IL-12p40−/− CD45.1^{+}	Bred in-house	N/A
Mouse: C57BL/6J	The Jackson Laboratory	Cat# 000664
Mouse B6.SJL-PtprcaPepcb/BoyJ	The Jackson Laboratory	Cat# 002014
Mouse: B6NTac	Taconic Biosciences	Cat# B6
Mouse: B6.SJL-Ptprca/BoyAiTac	Taconic Biosciences	Cat# 4007
Mouse: B6 1x2	Bred in-house	N/A
Mouse: B6.129S1-Il12a^{tm1Jm}/J	The Jackson Laboratory	Cat# 002692
Mouse: B6.Cg-Ptprca Pepcb Tg(TcrLCMV)1Aox/PpmJ	The Jackson Laboratory	Cat# 030450
Software and algorithms		
FlowJo (v10.6.2)	BD Biosciences	https://www.flowjo.com/solutions/flowjo/downloads
Prism 7.05	GraphPad Software	https://www.graphpad.com/scientific-software/prism/
GTEx Portal	Broad Institute of MIT and Harvard	http://www.gtexportal.org/home/index.html

RESOURCE AVAILABILITY

Lead contact

Further information and requests for resources and reagents should be directed to and will be fulfilled by the Lead Contact, Dr. Nevil J. Singh (nsingh@som.umaryland.edu)

Materials availability

This study did not generate new unique reagents.

Data and code availability

This paper analyzes existing, publicly available data from the GTEx Portal. The Genotype-Tissue Expression (GTEx) Project was supported by the Common Fund of the Office of the Director of the National Institutes of Health, and by NCI, NHGRI, NHLBI, NIDA, NIMH, and NINDS. The data used for the analyses described in this manuscript were obtained from the GTEx Portal on 07/15/2020. Accession for these datasets are listed in the Key resources table.

This paper does not report original code.

Any additional information required to reanalyze the data reported in this paper is available from the lead contact upon request.

EXPERIMENTAL MODEL AND SUBJECT DETAILS

Mice

Wild-type mice were obtained from both the Jackson Laboratory (C57BL/6J and B6.SJL-Ptprc^{a}Pepc^{b}/BoyJ) and Taconic Biosciences (B6NTac and B6.SJL-Ptprc^{a}/BoyAiTac). B6 mice were bred for dual congenic expression using a dam or sire from opposing place of purchase to eliminate any strain drift between the two wild-type strains. IL-12p40−/− (B6.129S1-*Il12bt*^{m1Jm}/J) and IL-12p35−/− (B6.129S1-*Il12at*^{m1Jm}/J) were sourced from the Jackson Laboratory. IL-12p40−/− mice were backcrossed to wild-type mice (B6.SJL-PtprcaPepcb/BoyJ) to generate CD45.1 congenic IL-12p40−/− mice. SMARTA TCR transgenic mice were obtained from Jackson Laboratories (B6.Cg-Ptprca Pepcb Tg(TcrLCMV)1Aox/PpmJ). For all experiments, both female and male mice between 4 and 35 weeks of age were used. Animals were bred and maintained under specific pathogen free (SPF) conditions at the University of Maryland, Baltimore. Experiments were performed with animals at least four weeks of age for bone marrow isolation and six weeks of age for all other experiments and approved by the University of Maryland, Baltimore Institutional Animal Care and Use Committee.

Parasite lines

A stable transfected line of the *Leishmania major* FV1 strain expressing a red fluorescent protein was generated as described previously (Kimblin et al., 2008). Briefly, the DsRed gene was amplified by PCR using the pCMV-DsRed-Express plasmid (BD Biosciences/Clontech) as a template and cloned into the SpeI site of the pKSNEO Leishmania expression plasmid. Promastigotes were transfected with the resulting expression plasmid construct [pKSNEO-DsRed] and selected for growth in the presence of 50 μg/ml Geneticin (G418) (Sigma). The resulting parasites are referred to as dsRed *L. major*. dsRed *L. major* fluoresces brightly and grows and infects flies and mice normally. *L. major*-DsRed promastigotes were grown at 25°C in medium 199 (GIBCO) supplemented with 20% heat-inactivated FCS, 15 mM HEPES, 0.1 mM adenine (in 50 mM HEPES), 5 μg/ml hemin (in 50% triethanolamine), and 0.6 μg/ml biotin (in 95% ethanol) (*Leish* media) and were split into new media every 2-3 days depending on amount of promastigotes in culture.

METHOD DETAILS

Generation of bone marrow chimeras

Femurs and tibias were taken from CD45.2^{+} IL-12p40−/−, CD45.1^{+} IL-12p40−/−, CD45.2^{+} IL-12p35−/− and CD45.1^{+}CD45.2^{+} B6 mice. The bone marrow was flushed out with a syringe and passed through a 100μm nylon mesh to generate a single cell suspension in 1X PBS supplemented with 5% FCS. Red blood cells were removed from suspension by Ficoll Paque Plus density gradient. Cells were washed twice and resuspended at 50 × 10^{6} cells/ml. Recipient IL-12p40−/− and IL-12p35−/− mice were irradiated with two doses of 600 rad before 5 x10^{6} bone marrow cells were transferred i.v. The mice rested for 6 weeks for cellular reconstitution.

Preparation of soluble *Leishmania* antigen

Soluble *Leishmania* antigen (SLA) was prepared from late-log-phase promastigotes of *L. major* after several passages in liquid culture. Promastigotes were harvested and counted and adjusted to 2x10^{8} promastigotes/mL. The promastigote suspension was washed three times in 5 mL sterile, cold phosphate-buffered saline (PBS). The suspension underwent five cycles of flash freezing in LN_2 and thawing followed by a centrifugation at 8,000 x g for 20 minutes at 4°C. Supernatant containing SLA was collected and protein concentration was determined by BCA assay (Pierce).

Leishmania infection of animals

Infective-stage promastigotes (metacyclics) were isolated from stationary cultures using peanut lectin agglutinin. Mice were infected in the footpad dermis with 10^6 metacyclic promastigotes in 20 μL using a 27-gauge 1/2 needle. Infection was monitored every 3-4 days by caliper measurement of lesion swelling. To characterize infection site leukocytes, footpad dermal tissue was digested in 1mL 2.5 mg/mL Collagenase D solution in complete RPMI at 37°C for 2 hours and filtered through a 70μm filter. For *in vitro* re-stimulation, cells were incubated in T cell media alone or separately with 50μg SLA for 48hr.

Adoptive transfer and antigen challenge

Lymph nodes were isolated from SMARTA TCR-tg and mechanically dissociated by mashing tissues through 70 μM nylon mesh. Red blood cells were removed from suspension using Ficoll Paque Plus density gradient. Cell suspension was further enriched for CD4+ T cells using Dynabeads Negative Selection. 100,000 cells were transferred into recipient animals and 24 hours later were challenged with 25μg LCMV GP_{61-80} peptide (Anaspec) and 5μg LPS or PBS as a control. Spleen tissue was isolated 5d post challenge and analyzed via flow cytometry for SMARTA cell numbers. Cells were set up for *in vitro* re-challenge in RPMI-1640 (GIBCO) supplemented with 10% FCS (Gemini), 1% sodium pyruvate (GIBCO), 1% antibiotic-antimycotic (GIBCO) and 0.000014% 2-mercaptoethanol (T cell media) alone or doses of LCMV GP_{61-80} peptide (1μg, 3μg, 10μg), normalized to SMARTA cell numbers, and analyzed 48hr later for cytokine production.

Tissue preparation

Single cell suspensions were prepared from the draining popliteal lymph node, non-draining popliteal lymph node, and spleen by dissociation and passage through 40μm nylon mesh. Lymphocytes were isolated for characterization from the liver, lung and footpad lesions through digestion in 1mL 2.5 mg/mL Collagenase D solution in T cell media at 37°C for 2hr followed by crushing through a 40μm cell strainer.

Intracellular stain and flow cytometry analysis

Single cell suspensions from tissue preparation were re-stimulated with 100ng/ml PMA and 1μg/ml Ionomycin in T cell media for 2 hours at 37°C and treated with 10μg/ml Brefeldin A (eBioscience) for an additional 4 hours at 37°C. For staining, Fc receptor blocking was performed for 15 minutes at 4°C in 1X PBS supplemented with 2% FCS, 0.01% azide, and 1% of each mouse, hamster and rat serums (Fc Block). Surface staining was performed for 30 minutes at 4°C in PBS supplemented with 2% FCS, 0.01% azide and 0.02% EDTA (FACS Buffer) using the antibodies listed. Cells were washed once with FACS buffer. Cells were fixed and permeabilized in BD Cytofix/Cytoperm solution for 20 minutes at 4°C, followed by an overnight incubation at 4°C in 1X eBioscience Fixation/Permeabilization Solution. Intracellular staining was performed using the antibodies described above in 1X eBioscience Permeabilization Buffer for 1 hour at 4°C. Stained cells were washed twice with 1X eBioscience Permeabilization Buffer followed by an additional two washes with FACS buffer. Cells were analyzed on the BD LSR-II cytometer and all data was analyzed using FlowJo (BD Biosciences). Antibodies used in these experiments are listed in the Key resources table.

Parasite quantification

Parasite load was quantified through limiting dilution. Tissues were processed as described above and homogenate was plated in triplicate in serial 10-fold dilutions in 96 well round bottom plates (Corning) containing *Leish* media. Plates were incubated at 25°C for 10 days, at which point the number of viable parasites was determined microscopically. Total parasite burden was calculated from the highest dilution at which promastigotes could be detected.

Live parasite analysis by flow cytometry

Animals were infected as described above and the infection allowed to proceed for 22 days. At the endpoint, tissues were harvested and processed as described above in preparation for flow cytometry analysis. Once tissues were in single cell suspension, surface staining was done in 1X PBS at 25°C for 10min, followed by propidium iodide (Sigma) staining at 10ug/mL in 1X PBS for 10min at 25°C in the dark. Cells were analyzed on the BD LSR-II cytometer and all data was analyzed using FlowJo (BD Biosciences). Antibodies used for this experiment are listed in the Key resources table.

Cytokine production quantification

Tissue samples were processed as described above and single cell suspensions were plated in triplicate in 96-well plates (Corning). Levels of IL-17A and IFNγ in supernatants were assessed by sandwich enzyme-linked immunosorbent assay (ELISA) by using the Ready-SET-Go! systems (eBioscience). IL-12p40, IL-12p70, IL-2 and IL-4 were measured using Quantikine ELISA systems (R&D Systems).

QUANTIFICATION AND STATISTICAL ANALYSIS

All data analyzed in this study was analyzed using GraphPad Prism software, version 7.05. Information about specific statistical tests used for each experiment are listed in the figure legends.

Cell Reports, Volume *37*

Supplemental information

The subunits of IL-12, originating from two distinct cells, can functionally synergize to protect against pathogen dissemination *in vivo*

Allison N. Gerber, Kaveh Abdi, and Nevil J. Singh

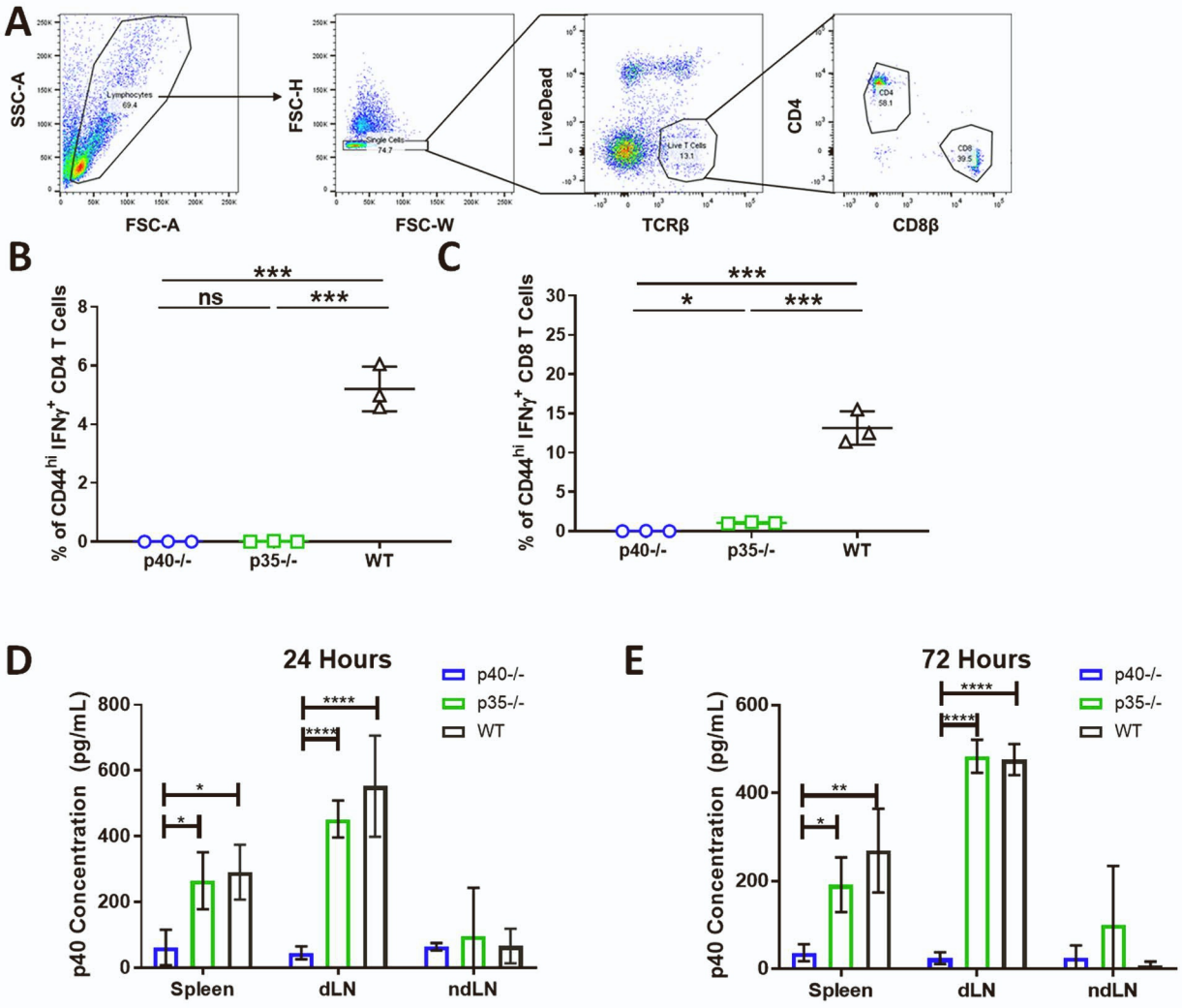

Figure S1. Supplemental Data for Figure 1

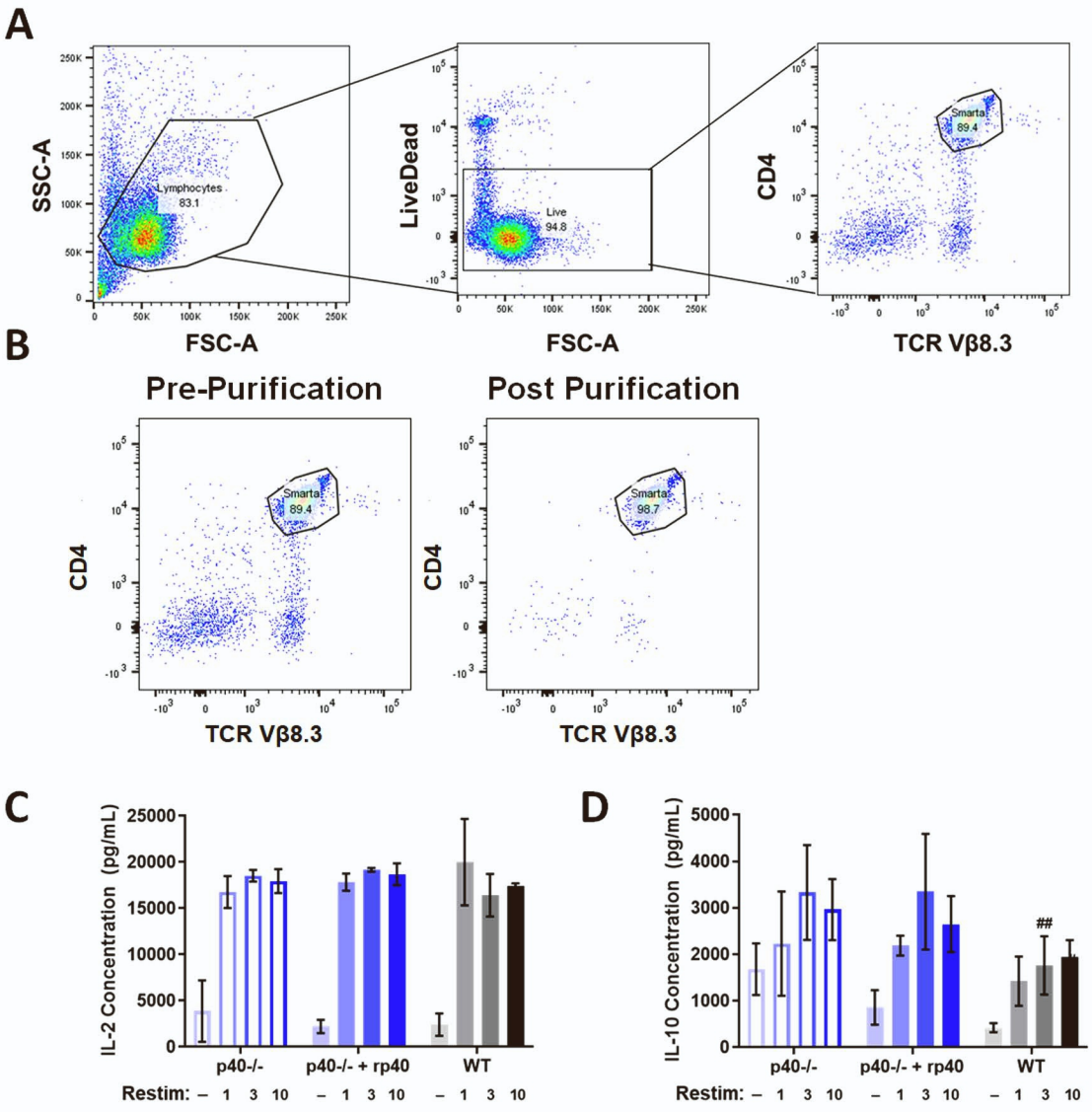

Figure S2. Supplemental Data for Figure 2

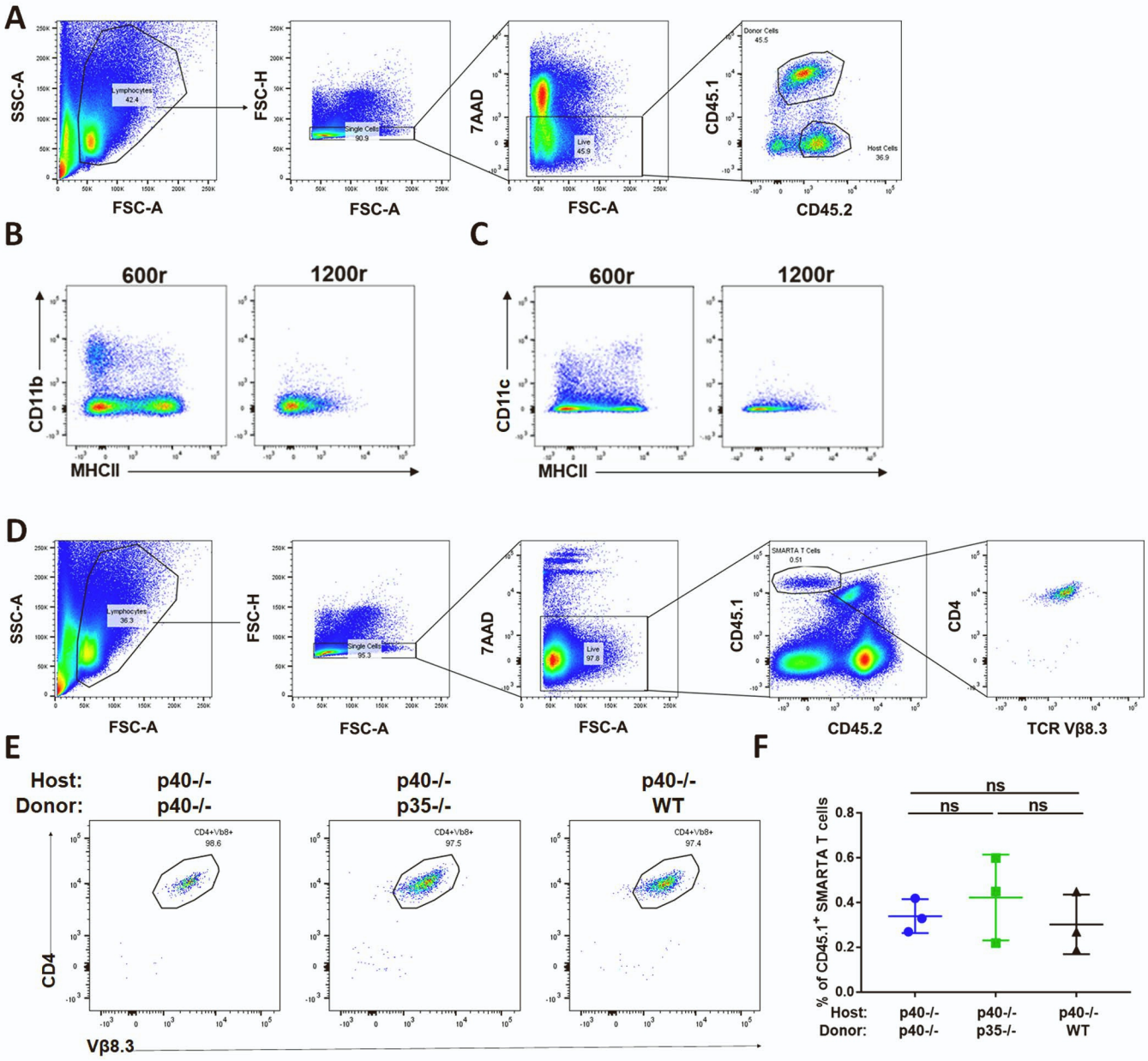

Figure S3. Supplemental Data for Figure 3

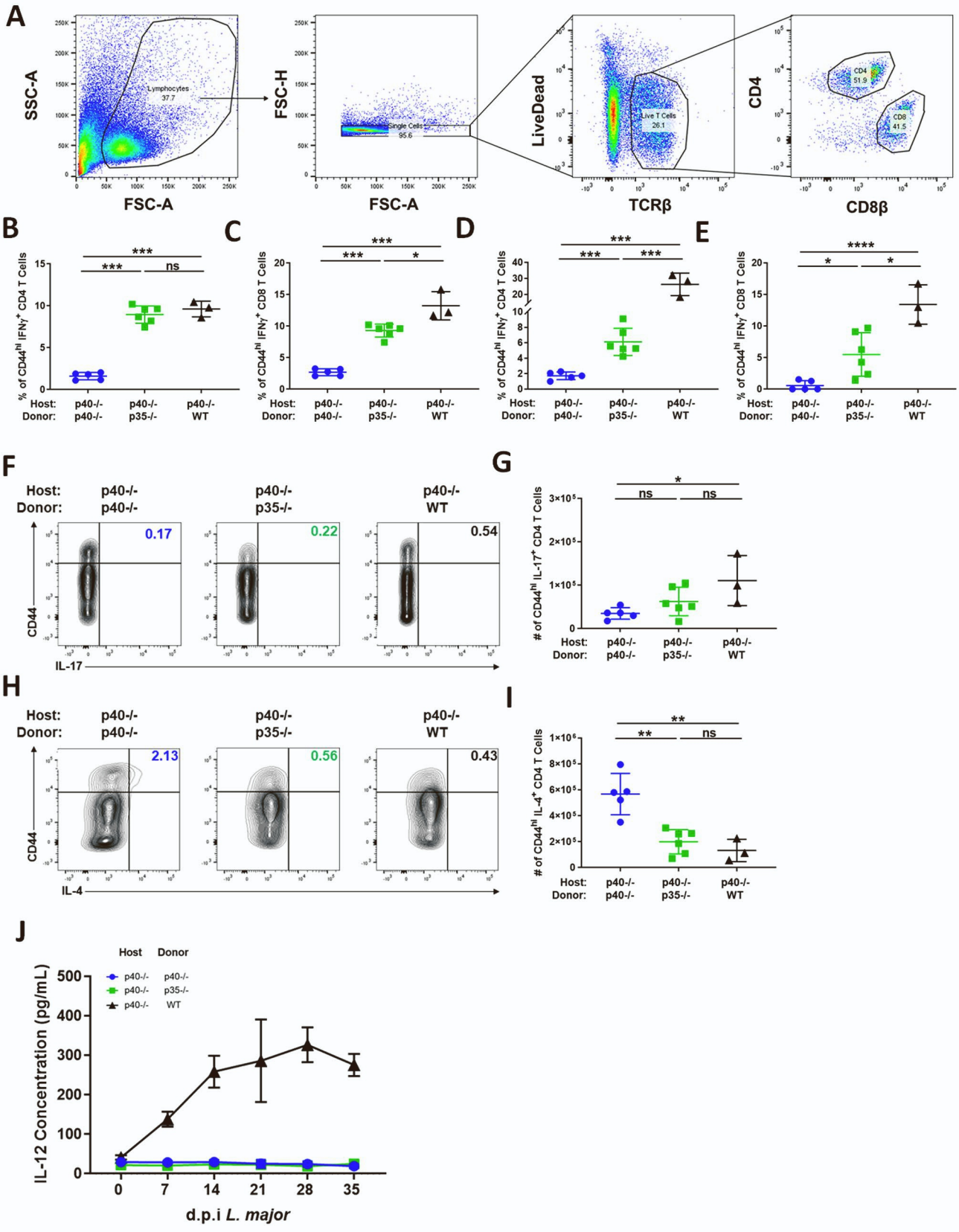

Figure S4. Supplemental Data for Figure 4

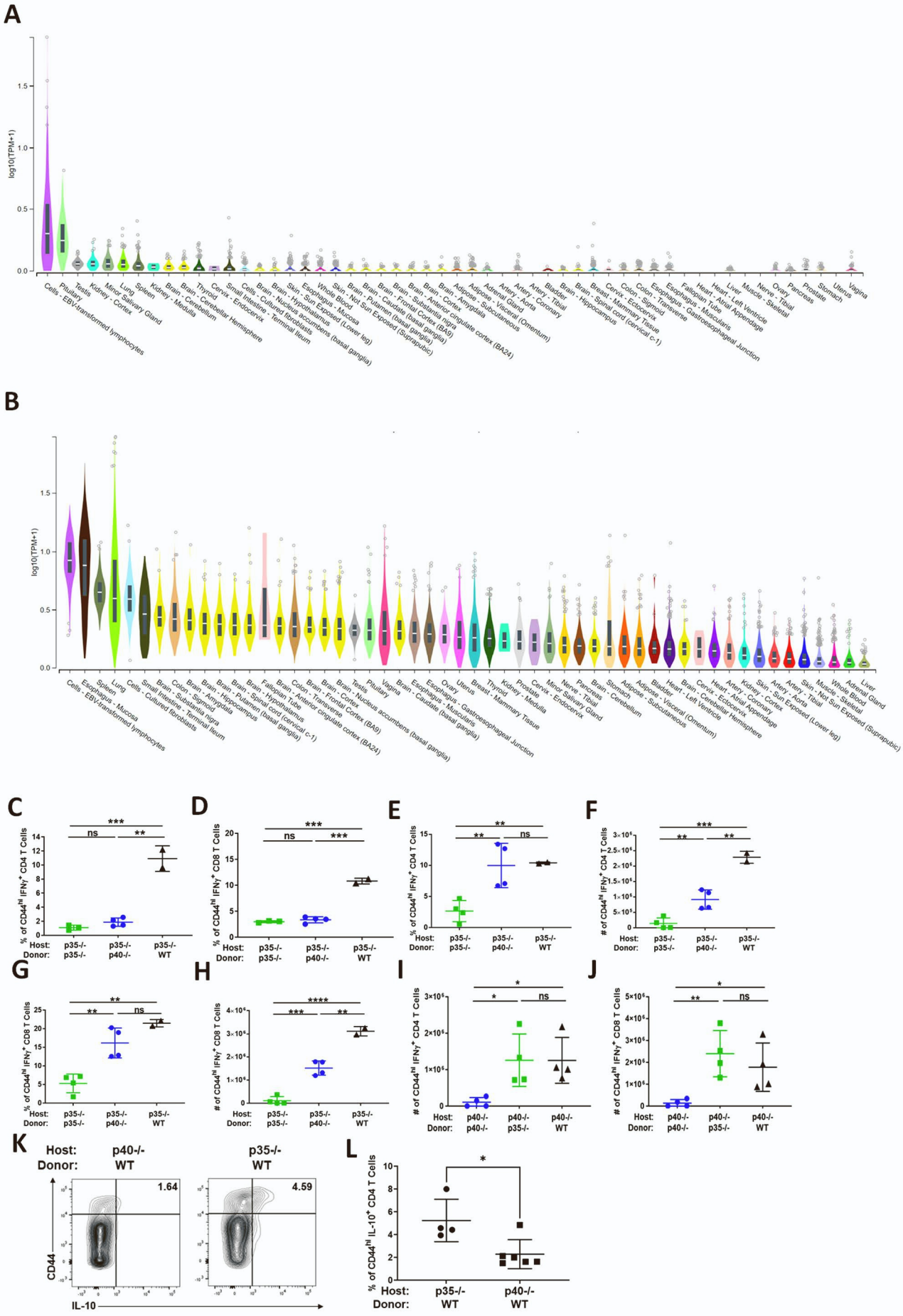

Figure S5. Supplemental Data for Figure 5

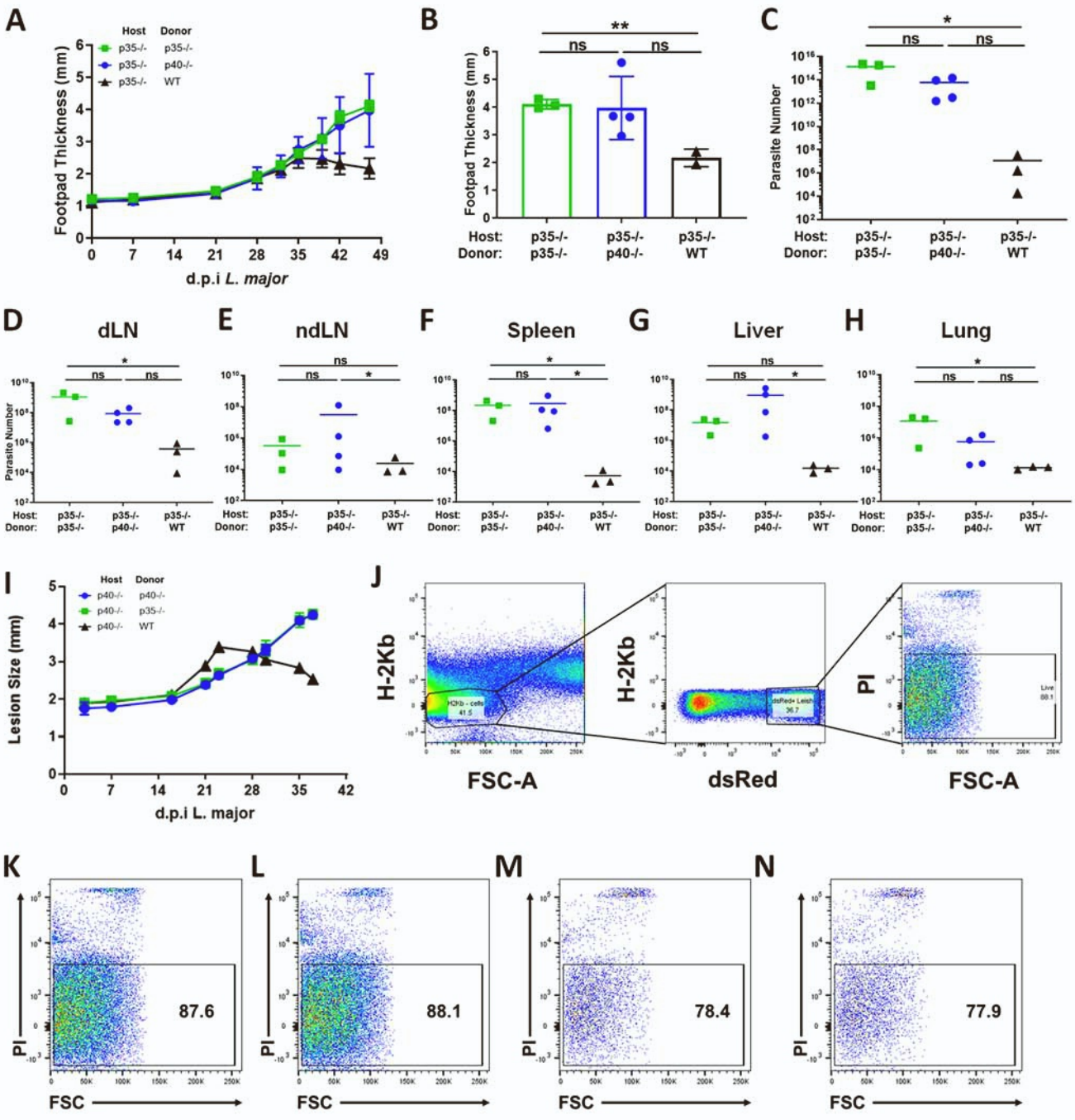

Figure S6. Supplemental Data for Figure 6

Supplemental Information

Figure S1. T cell differentiation is disrupted in p40-/- and p35-/- mice. Related to Figure 1.

(**A**) Gating strategy used for Figure 1D-G

(**B**) Percentage of $CD44^{hi}$ $IFN\gamma^{+}$ $CD4^{+}$ T cells in the spleen of p40-/- (open circles, blue), p35-/- (open squares, green) and WT (open triangles, black) animals measured 28 days after infection (unpaired t test, n=3)

(**C**) Same as in (**B**) but $CD8^{+}$ T cells(unpaired t test, n=3)

(**D-E**) Cells from the spleen, draining lymph node (dLN) and non-draining lymph node (ndLN) were harvested 28 days after infection and incubated *in vitro*. Concentration of p40 in supernatants by tissues collected from p40-/- (blue), p35-/- (green) and WT (black, shaded) after (**D**) 24 and (**E**) 72 hours. (unpaired t test, n=3)

Data from this figure are representative of two independent experiments where the n indicates biological replicates. (B-E) are displayed as mean ± SEM. Significance is indicated as follows: $p<0.05$ = * ; $p<0.01$ = ** ; $p<0.001$ = *** ; $p<0.0001$ = ****. Anything not marked is considered not statistically significant

Figure S2. Purification of SMARTA T cells and cytokine production in response to rp40 administration, related to Figure 2

(**A**) Gating strategy used to verify purity of SMARTA-tg T cells in Figure 2.

(**B**) Purity of SMARTA-tg T cells after Dynabead Magnetic Sorting

(**C-D**) Splenocytes harvested 5 days after challenge were normalized to SMARTA T cell number and re-stimulated in vitro with GP_{61-80} for 48h. Re-stimulation doses are in µg. Concentration of (**C**) IL-2, and (**D**) IL-10 in supernatant from splenocytes of SMARTA T cells transferred into p40-/- animals treated with PBS (left, blue open bars) p40-/- animals given 1µg recombinant p40 (middle, blue closed bars) or WT animals (right, gray bars)

Data from this figure are representative of one independent experiment where the n indicates biological replicates. (C-D) are displayed as mean ± SEM. Significance is indicated as follows: $p<0.05$ = * ; $p<0.01$ = ** ; $p<0.001$ = *** ; $p<0.0001$ = ****. Anything not marked is considered not statistically significant.

Figure S3. SMARTA T cell adoptive transfer into reconstituted p40-/- host chimeric animals, related to Figure 3

(**A-C**) Bone marrow chimeras were generated by reconstituting $CD45.2^{+}$ p40-/- mice that were irradiated with either one or two doses of 600rad with bone marrow cells from $CD45.1^{+}CD45.2^{+}$ WT donor mice. Chimeric mice were analyzed for host cell depletion after a 6 week reconstitution period.

(**A**) Gating strategy for Supplemental Figure 2C-D

(**B**) $CD45.2^{+}$ host cell expression of $CD11b^{+}$ and $MHCII^{+}$ in chimeric animals that were irradiated with 600r (left) versus 1200r (right)

(**C**) $CD45.2^{+}$ host cell expression of CD11c and MHCII in chimeric animals that were irradiated with 600r (left)

versus 1200r (right)

(**D**) Gating strategy for Figure 2B

(**E**) Frequency of $CD4^+V\beta8.3^+$ T cells in Donor SMARTA gates shown in Figure 2B

(**F**) Frequencies of transferred SMARTA T cells in spleens of recipient chimeras 5 days after challenge (n=3).

Data from this figure are representative of one independent experiment where n indicates the number of biological replicates. (F) is displayed as mean ± SEM. Significance is indicated as follows: $p<0.05$ = * ; $p<0.01$ = ** ; $p<0.001$ = *** ; $p<0.0001$ = ****. Anything not marked is considered not statistically significant.

Figure S4. Cytokine responses by T cells in the presence or absence of two-cell IL-12, related to Figure 4

(**A**) Gating strategy used for Figure 3

(**B**) Percentage of $CD44^{hi}$ $IFN\gamma^+$ CD4+ T cells in the spleen of p40-/- host chimeras reconstituted with p40-/- (circles, blue), p35-/- (squares, green) or WT (triangles, black) donor bone marrow 35 days after infection (unpaired t test, p40-/-→p40-/- n =4; p35-/-→p40-/- n=6; WT→p40-/- n=3)

(**C**) Same as in (**B**) but $CD8^+$ T Cells (unpaired t test, n=3-6)

(**D**) Percentage of $CD44^{hi}$ $IFN\gamma^+$ CD4+ T cells in lymphocytes harvested from the footpad lesion of p40-/- host chimeras reconstituted with p40-/- (circles, blue) p35-/- (squares, green) or WT (triangles, black) donor bone marrow 35 days after infection (unpaired t test, p40-/-→p40-/- n =4; p35-/-→p40-/- n=6; WT→p40-/- n=3).

(**E**) Same as in (**D**) but CD8 T cells (unpaired t test, p40-/-→p40-/- n =4; p35-/-→p40-/- n=6; WT→p40-/- n=3).

(**F**) Percentage and (**G**) Number of $CD44^{hi}$ IL-17^+ CD4 T cells in the spleen of p40-/- host chimeras reconstituted with p40-/- (circles, blue), p35-/- (squares, green) or WT (triangles, black) donor bone marrow 35 days after infection (unpaired t test, p40-/-→p40-/- n =4; p35-/-→p40-/- n=6; WT→p40-/- n=3)

(**H**) Percentage and (**I**) Number of $CD44^{hi}$ IL-4^+ CD4 T cells in the spleen of p40-/- host chimeras reconstituted with p40-/- (circles, blue), p35-/- (squares, green) or WT (triangles, black) donor bone marrow 35 days after infection (unpaired t test, p40-/-→p40-/- n =4; p35-/-→p40-/- n=6; WT→p40-/- n=3)

(**J**) Infected animals were bled prior to infection (d0), and at d7, d14, d21, d28 and d35 post infection. Serum IL-12 levels for p40-/- host chimeras reconstituted with p40-/- (circles, blue) p35-/- (squares, green), and WT (triangles, black) animals were measured by ELISA (p40-/-→p40-/- n =4; p35-/-→p40-/- n=6; WT→p40-/- n=3).

Data from this figure are representative of two independent experiments where the n indicates the number of biological replicates. (B-E, G, I-J) are displayed as mean ± SEM. Significance is indicated as follows: $p<0.05$ = * ; $p<0.01$ = ** ; $p<0.001$ = *** ; $p<0.0001$ = ****. Anything not marked is considered not statistically significant.

Figure S5. Hematopoietic cell expression of p40 is critical for two-cell IL-12 formation, related to Figure 5

(**A**) GTEx Portal analysis for expression levels of p40 throughout different tissues

(**B**) GTEx Portal analysis for expression levels of p35 throughout different tissues

(**C-D**) Bone marrow chimeras were generated by reconstituting $CD45.2^+$ p35-/- mice irradiated with 1200rad with bone marrow cells from $CD45.1^+$ p40-/-, $CD45.2^+$ p35-/- or $CD45.1^+CD45.2^+$ WT donor mice. Chimeric mice were

infected in the footpad dermis with 10^6 dsRed *L. major* parasites following reconstitution. 35 days after infection, tissues were harvested and restimulated for intracellular cytokine staining and flow cytometry analysis. Gating strategy used for these panels is shown in Supplemental Figure 3A

(**C**) Percentage of $CD44^{hi}$ $IFN\gamma^+$ $CD4^+$ T cells in the spleen of 1200r p35-/- host chimeras reconstituted with p35-/- (squares, green), p40-/- (circles, blue) or WT (triangles, black) donor bone marrow 35 days after infection (unpaired t test, p35-/-→p35-/- n=3; p40-/-→p35-/- n=4; WT→p35-/- n=2)

(**D**) Same as in (**C**) but CD8 T cells (unpaired t test, p35-/-→p35-/- n=3; p40-/-→p35-/- n=4; WT→p35-/- n=2)

(**E-H**) Bone marrow chimeras were generated by reconstituting $CD45.2^+$ p35-/- mice irradiated with 600rad with bone marrow cells from $CD45.1^+$ p40-/-, $CD45.2^+$ p35-/- or $CD45.1^+CD45.2^+$ WT donor mice. Chimeric mice were infected in the footpad dermis with 10^6 dsRed *L. major* parasites following reconstitution. 35 days after infection, tissues were harvested and restimulated for intracellular cytokine staining and flow cytometry analysis. Gating strategy used for these panels is shown in Supplemental Figure 3A

(**E**) Percentage and (**F**) Number of $CD44^{hi}$ $IFN\gamma^+$ $CD4^+$ T cells in the spleen of 600r p35-/- host chimeras reconstituted with p35-/- (squares, green), p40-/- (circles, blue) or WT (triangles, black) donor bone marrow 35 days after infection (unpaired t test, p35-/-→p35-/- n=3; p40-/-→p35-/- n=4; WT→p35-/- n=2)

(**G**) Same as in (**E**) but $CD8^+$ T cells (unpaired t test, p35-/-→p35-/- n=3; p40-/-→p35-/- n=4; WT→p35-/- n=2)

(**H**) Same as in (**F**) but $CD8^+$ T cells (unpaired t test, p35-/-→p35-/- n=3; p40-/-→p35-/- n=4; WT→p35-/- n=2)

(**I**) Number of $CD44^{hi}$ $IFN\gamma^+$ $CD4^+$ T cells in the spleen of 600r p40-/- host chimeras reconstituted with p40-/- (circles, blue), p35-/- (squares, green) or WT (triangles, black) donor bone marrow 35 days after infection (unpaired t test, n=4)

(**J**) Same as in (**I**) but $CD8^+$ T cells (unpaired t test, n=4)

(**K-L**) Percentage of $CD44^{hi}$ IL-10^+ CD4+ T cells in the spleen of p35-/- or p40-/- host chimeras reconstituted with WT bone marrow 35 days after infection (unpaired t test, n=4-6).

Data from this figure is representative of two independent experiments where the n refers to the number of biological replicates. (C-J, L) are displayed as mean ± SEM. Significance is indicated as follows: $p<0.05$ = * ; $p<0.01$ = ** ; $p<0.001$ = *** ; $p<0.0001$ = ****. Anything not marked is considered not statistically significant.

Figure S6. Control of *L. major* parasite burden in p35-/- host chimeric animals, related to Figure 6

(**A-H**) Bone marrow chimeras were generated by reconstituting irradiated $CD45.2^+$ p35-/- mice with bone marrow cells from $CD45.1^+$ p40-/-, $CD45.2^+$ p35-/- or $CD45.1^+CD45.2^+$ WT donor mice. Chimeric mice were infected in the footpad dermis with 10^6 dsRed *L. major* parasites following reconstitution.

(**A**) Biweekly measurement of footpad thickness at the midline following establishment of visible lesion for p35-/- host chimeras reconstituted with p35-/- (squares, green), p40-/- (circles, blue) or WT (triangles, black) through the duration of infection (p35-/-→p35-/- n=3; p40-/-→p35-/- n=4; WT→p35-/- n=2)

(**B**) Footpad thickness at the midline of p35-/- host chimeras reconstituted with p35-/- (squares, green), p40-/- (circles, blue) or WT (triangles, black) 35 days post infection (p35-/-→p35-/- n=3; p40-/-→p35-/- n=4; WT→p35-/- n=2)

(**C-H**) dsRed *L. major* parasite quantified by limiting dilution from (**C**) footpad lesion, (**D**) draining popliteal lymph node (dLN), (**E**) non-draining popliteal lymph node (ndLN), (**F**) spleen, (**G**) liver and (**H**) lung tissue of p35-/- host chimeras reconstituted with p35-/- (squares, green), p40-/- (circles, blue) or WT (triangles, black) 35 days post infection (unpaired t test, p35-/-→p35-/- n=3; p40-/-→p35-/- n=4; WT→p35-/- n=2)

(**I**) Bone marrow chimeras infected with 10^6 WT *L. major* parasite for comparison to chimeras infected with dsRed *L. major* parasite in Figure 6A. (n=4)

(**J-N**) p40-/- animals were infected with dsRed *L. major* in the footpad dermis. Following 22 days, tissues were harvested and stained for the presence of live, dsRed parasites via flow cytometry. (**J**) Gating strategy to differentiate live and dead dsRed *L. major* in different tissues during infection. Cells were gated on $H2Kb^-$, small cells that were $dsRed^+$ and viability measured by PI staining. The proportion of live dsRed+ parasites in the (**K**) lymph node, (**L**) spleen, (**M**) lung and (**N**) liver is shown.

Data from this figure is representative of two independent experiments where the n refers to the number of biological replicates. (A-I) are displayed as mean ± SEM. Significance is indicated as follows: $p<0.05$ = * ; $p<0.01$ = ** ; $p<0.001$ = *** ; $p<0.0001$ = ****. Anything not marked is considered not statistically significant.